

THE ASSEMBLY AND MERGING HISTORY OF SUPERMASSIVE BLACK HOLES IN HIERARCHICAL MODELS OF GALAXY FORMATION

MARTA VOLONTERI,^{1,2} FRANCESCO HAARDT,² AND PIERO MADAU³

Received 2002 July 2; accepted 2002 September 10

ABSTRACT

We assess models for the assembly of supermassive black holes (SMBHs) at the center of galaxies that trace their hierarchical buildup far up in the dark halo “merger tree.” Motivated by the recent discovery of luminous quasars around redshift $z \approx 6$ —suggesting a very early assembly epoch—and by numerical simulations of the fragmentation of primordial molecular clouds in cold dark matter (CDM) cosmogonies, we assume that the first “seed” black holes (BHs) had intermediate masses and formed in (mini)halos collapsing at $z \sim 20$ from high- σ density fluctuations. As these pregalactic holes become incorporated through a series of mergers into larger and larger halos, they sink to the center because of dynamical friction, accrete a fraction of the gas in the merger remnant to become supermassive, form a binary system, and eventually coalesce. The merger history of dark matter halos and associated BHs is followed by cosmological Monte Carlo realizations of the merger hierarchy from early times until the present in a Λ CDM cosmology. A simple model, where quasar activity is driven by major mergers and SMBHs accrete at the Eddington rate a mass that scales with the fifth power of the circular velocity of the host halo, is shown to reproduce the observed luminosity function of optically selected quasars in the redshift range $1 < z < 5$. A scheme for describing the hardening of a BH binary in a stellar background with core formation due to mass ejection is applied, where the stellar cusp proportional to r^{-2} is promptly regenerated after every major merger event, replenishing the mass displaced by the binary. Triple BH interactions will inevitably take place at early times if the formation route for the assembly of SMBHs goes back to the very first generation of stars, and we follow them in our merger tree. The assumptions underlying our scenario lead to the prediction of a population of massive BHs wandering in galaxy halos and the intergalactic medium at the present epoch and contributing $\lesssim 10\%$ to the total BH mass density, $\rho_{\text{SMBH}} = 4 \times 10^5 M_{\odot} \text{ Mpc}^{-3}$ ($h = 0.7$). The fraction of binary SMBHs in galaxy nuclei is on the order of 10% today, and it increases with redshift so that almost all massive nuclear BHs at early epochs are in binary systems. The fraction of binary quasars (both members brighter than $0.1L_*$) instead is less than 0.3% at all epochs. The nuclear SMBH occupation fraction is unity (0.6) at the present epoch if the first seed BHs were as numerous as the 3.5σ (4σ) density peaks at $z = 20$.

Subject headings: black hole physics — cosmology: theory — galaxies: evolution — quasars: general

1. INTRODUCTION

Dynamical evidence indicates that supermassive black holes (SMBHs) reside at the center of most nearby galaxies (Richstone et al. 1998). The available data show an empirical correlation between bulge luminosity and black hole (BH) mass (Magorrian et al. 1998), which becomes remarkably tight when the stellar velocity dispersion of the host bulge, σ_c , is plotted instead of luminosity (Ferrarese & Merritt 2000; Gebhardt et al. 2000). The $m_{\text{BH}}\text{--}\sigma_c$ relation implies a rough proportionality between SMBH mass and the mass of the baryonic component of the bulge. It is not yet understood if this relation was set in primordial structures and, consequently, how it is maintained throughout cosmic time with such a small dispersion or, indeed, which physical processes established such a correlation in the first place (e.g., Silk & Rees 1998; Haehnelt & Kauffmann 2000; Adams, Graff, & Richstone 2001; Burkert & Silk 2001). Most recently, it has been shown by Ferrarese (2002) that in elliptical and spiral galaxies the bulge velocity dispersion correlates tightly with the value of the circular velocity measured well beyond the optical radius, suggesting that m_{BH} is

actually determined by the mass of the host dark matter halo.

The strong link between the masses of SMBHs and the gravitational potential wells that host them suggests a fundamental mechanism for assembling BHs and forming spheroids in galaxy halos. In popular cold dark matter (CDM) “bottom-up” cosmogonies, small-mass subgalactic systems form first to merge later into larger and larger structures. Galaxy halos then experience multiple mergers during their lifetime, with those between comparable mass systems (“major mergers”) expected to result in the formation of elliptical galaxies (see, e.g., Barnes 1988; Hernquist 1992). Simple models in which SMBHs are also assumed to grow during major mergers and to be present in every galaxy at any redshift—while only a fraction of them are “active” at any given time—have been shown to explain many aspects of the observed evolution of quasars (e.g., Cattaneo, Haehnelt, & Rees 1999; Cavaliere & Vittorini 2000; Kauffmann & Haehnelt 2000; Wyithe & Loeb 2002). In hierarchical structure formation scenarios, the ubiquity of SMBHs in nearby luminous galaxies can arise even if only a small fraction of halos harbor SMBHs at high redshift (Menou, Haiman, & Narayanan 2001). Yet several important questions remain unanswered:

1. Did the first massive BHs form in subgalactic units far up in the merger hierarchy, well before the bulk of the stars

¹ Dipartimento di Fisica, Università di Milano, Bicocca, Italy.

² Dipartimento di Scienze, Università dell’Insubria/Sede di Como, Italy.

³ Department of Astronomy and Astrophysics, University of California at Santa Cruz, 1156 High Street, Santa Cruz, CA 95064.

observed today? The seeds of the recently discovery $z \approx 6$ quasars in the Sloan Digital Sky Survey (SDSS; Fan et al. 2001b) had to appear at very high redshift, $z \gtrsim 10$, if the SDSS quasars are accreting no faster than the Eddington rate and are not gravitationally lensed or beamed (Haiman & Loeb 2001).

2. How massive were the initial BH seeds? A clue to this question might lie in the numerous population of ultraluminous off-nuclear (“non-AGN”) X-ray sources (ULXs) that have been detected in nearby galaxies (e.g., Colbert & Mushotzky 1999; Makishima et al. 2000; Kaaret et al. 2001). Assuming isotropic emission, the inferred masses of these ULXs often suggest intermediate-mass BHs with $m_{\bullet} \gtrsim$ a few hundred M_{\odot} .

3. How efficiently do SMBHs and their “seeds” spiral inward and coalesce as they get incorporated through a series of mergers into larger systems? And what is the cumulative dynamical effect of multiple BH mergers on galaxy cores?

4. Is there a population of relic “Population III” massive holes lurking in present-day galaxy halos?

In this paper we explore a formation route for the assembly of SMBHs in the nuclei of galaxies that traces their seeds back to the very first generation of stars, in (mini)halos above the cosmological Jeans mass collapsing at $z \sim 20$ from the high- σ peaks of the primordial density field. The first stars must have formed out of metal-free gas, with the lack of an efficient cooling mechanism possibly leading to a very top-heavy initial stellar mass function (IMF; Larson 1998) and, in particular, to the production of very massive stars (VMSs) with $m_{*} > 100 M_{\odot}$ (Carr, Bond, & Arnett 1984). Recent numerical simulations of the fragmentation of primordial clouds in standard CDM theories all show the formation of Jeans-unstable clumps with masses exceeding a few hundred solar masses; because of the slow subsonic contraction—a regime set up by the main gas coolant, molecular hydrogen—further fragmentation into subcomponents is not seen (Bromm, Coppi, & Larson 1999, 2002; Abel, Bryan, & Norman 2000). Moreover, the different conditions of temperature and density of the collapsing cloud result in a mass accretion rate over the hydrostatic protostellar core $\sim 10^3$ times larger than that observed in local forming stars, suggesting that Population III stars were indeed very massive (Omukai & Nishi 1998; Ripamonti et al. 2002). If VMSs form above $260 M_{\odot}$, after 2 Myr they would collapse to massive BHs containing at least half of the initial stellar mass (Fryer, Woosley, & Heger 2001), i.e., with masses intermediate between those of the stellar and supermassive variety. It has been suggested by Madau & Rees (2001, hereafter MR01) that a numerous population of massive BHs may have been the end-product of the first episode of pregalactic star formation; since they form in high- σ rare density peaks, relic massive BHs with $m_{\bullet} \gtrsim 150 M_{\odot}$ would be predicted to cluster in the cores of more massive halos formed by subsequent mergers.

In this paper we expand upon the original suggestion of MR01 and assess a model for the assembly of SMBHs in the nuclei of luminous galaxies out of accreting Population III seed holes. The merger history of dark matter halos and associated BHs is followed through Monte Carlo realizations of the merger hierarchy (merger trees). Merger trees are a powerful tool for tracking the evolution of SMBH binaries along cosmic time and analyzing how their fate is

influenced by the environment (e.g., stellar density cusps). We study the conditions under which pregalactic massive holes may sink to the halo center because of dynamical friction, accrete a fraction of the gas in the merger remnant to become supermassive, form a binary system, and eventually coalesce. Major mergers are frequent at early times, so a significant number of binary SMBH systems are expected to form then. To anticipate the results of our analysis, we find that a simple model where quasar activity is driven by major mergers and SMBHs accrete at the Eddington rate a mass that scales with the fifth power of the circular velocity of the host halo is able to reproduce the observed luminosity function (LF) of optically selected quasars in the redshift range $1 < z < 5$. Minor mergers are largely responsible for a population of isolated BHs wandering in galaxy halos, while intergalactic BHs will be produced by the gravitational slingshot—the ejection of one BH when three holes interact.

2. HALO MERGER TREE

There are now a number of algorithms for constructing merger trees, the difficulties and drawbacks of various techniques having been reviewed by Somerville & Kolatt (1999). We have developed a Monte Carlo algorithm similar in spirit to the one described by Cole et al. (2000) and based on the extended Press-Schechter (EPS) formalism. This gives the fraction of mass in a halo of mass M_0 at redshift z_0 , which at an earlier time was in smaller progenitors of mass in the range M to $M + dM$,

$$f(M, M_0) dM = \frac{1}{\sqrt{2\pi}} \frac{D}{S^{3/2}} \exp\left(-\frac{D^2}{2S}\right) \frac{d\sigma_M^2}{dM} dM, \quad (1)$$

where $D \equiv \delta_c(z) - \delta_c(z_0)$ and $S \equiv \sigma_M^2(z) - \sigma_{M_0}^2(z_0)$ (Bower 1991; Lacey & Cole 1993). Here $\sigma_M^2(z)$ and $\sigma_{M_0}^2(z_0)$ are the linear theory rms density fluctuations smoothed with a “top-hat” filter of mass M and M_0 at redshifts z and z_0 , respectively. The $\delta_c(z)$ and $\delta_c(z_0)$ are the critical thresholds on the linear overdensity for spherical collapse at the two redshifts. Integrating this function over the range $0 < M < M_0$ gives unity; all the mass of M_0 was in smaller subclumps at an earlier epoch $z > z_0$. Taking the limit $z \rightarrow z_0$ and multiplying by the factor M_0/M to convert from mass weighting to number weighting, equation (1) gives the number of progenitors the more massive halo fragments into when one takes a small step δz back in time,

$$\frac{dN}{dM}(z = z_0) = \frac{1}{\sqrt{2\pi}} \frac{M_0}{M} \frac{1}{S^{3/2}} \frac{d\delta_c}{dz} \frac{d\sigma_M^2}{dM} \delta z. \quad (2)$$

Our algorithm uses this expression to build a binary merger tree that starts from the present day and runs backward in time “disintegrating” a parent halo into its progenitors. Because for CDM-like power spectra the number of halos diverges as the mass goes to zero, it is necessary to introduce a cutoff mass or effective mass resolution M_{res} , which marks the transition from *progenitor*—all halos with $M > M_{\text{res}}$ —to *accreted mass*—the cumulative contribution of all halos with $M < M_{\text{res}}$ (Somerville & Kolatt 1999). Having specified the mass resolution, one can compute the mean number of fragments in the range $M_{\text{res}} < M < M_0/2$,

$$N_p = \int_{M_{\text{res}}}^{M_0/2} \frac{dN}{dM} dM, \quad (3)$$

and the fraction of accreted mass,

$$F_a = \int_0^{M_{\text{res}}} \frac{dN}{dM} \frac{M}{M_0} dM. \quad (4)$$

Both of these quantities are proportional to the time step δz , which is chosen to ensure that multiple fragmentation is unlikely, i.e., $N_p \ll 1$. Hence, it is the frequency of mergers that directly controls the time step; this enables the algorithm to follow the merger process with high time resolution. Following Cole et al. (2000), at every time step a random number $0 \leq R \leq 1$ is generated and compared to N_p . If $R \geq N_p$, the parent halo does not fragment in this time step, but its mass is reduced to account for the accreted matter; i.e., a new halo is produced with mass $M_0(1 - F_a)$. Fragmentation occurs instead if $R < N_p$; then a random value of M in the range $M_{\text{res}} < M < M_0/2$ is generated from the distribution in equation (2) to produce two new halos with masses M and $M_0(1 - F_a) - M$. The merger hierarchy is built up by repeating the same procedure on each subclump at successive time steps.

To fully define the tree we need to specify the power spectrum of density fluctuations, which gives the function σ_M , and the cosmological parameters Ω_0 and Ω_Λ , which the critical overdensity for collapse δ_c depends upon. Unless otherwise stated, all the results shown below refer to the currently favored (by a variety of observations) Λ CDM world model with $\Omega_0 = 0.3$, $\Omega_\Lambda = 0.7$, $h = 0.7$, $\Omega_b h^2 = 0.02$,

and $n = 1$. In this cosmology the redshift dependence of the matter density parameter is $\Omega(z) = \Omega_0(1+z)^3[1 - \Omega_0 + (1+z)^3\Omega_0]^{-1}$, and the linear theory growth factor is accurately approximated by

$$D(z) = \frac{5\Omega}{2(1+z)} \left(\frac{1}{70} + \frac{209}{140}\Omega - \frac{\Omega^2}{140} + \Omega^{4/7} \right)^{-1} \quad (5)$$

(Carroll, Press, & Turner 1992), so that $\sigma_M(z) = \sigma_M(0)D(z)/D(0)$. The normalization of the mass fluctuation spectrum, derived from the abundance of X-ray-emitting clusters observed in the local universe, is $\sigma_8(0) \equiv \sigma_0(r = 8 h^{-1} \text{ Mpc}) = 0.93$ (Eke, Cole, & Frenk 1996). We have used the fit to the CDM power spectrum given by Bardeen et al. (1986), modified to account for the effects of baryon density following Sugiyama (1995). For the spherical collapse density threshold δ_c we use the fit (accurate within 0.1% for $1 - \Omega > 0.01$) from Nakamura & Suto (1997), $\delta_c(z) = 1.686[1 + 0.012299 \log(1 - \Omega)]$.

All that remains to be fixed is the mass resolution and time step. We have taken M_{res} to represent at $z = 0$ a subclump with virial velocity equal to 10% that of the M_0 parent halo, i.e., $M_{\text{res}} = 10^{-3} M_0$; the mass resolution is taken to decrease with redshift as $(1+z)^{-3.5}$, so it is always less than 5% of the mass of the main halo in the merger hierarchy. This ensures a sufficiently wide range of masses to allow for both minor and major mergers in the tree at all redshifts. Because of the binary nature of the algorithm

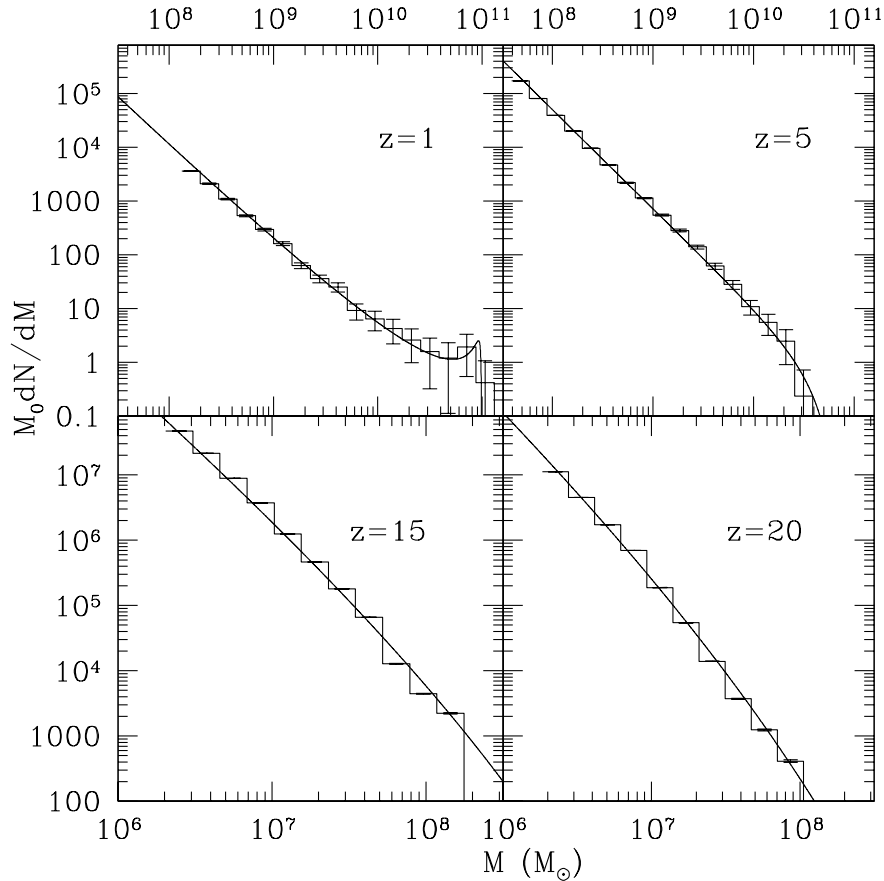


FIG. 1.—Mean number of progenitors with mass M for a $z_0 = 0$, $M_0 = 10^{11} M_\odot$ parent halo, at redshifts $z = 1, 5, 15$, and 20 . Solid lines are the predictions of the EPS theory; histograms show the results for the merger tree (mean of 50 realizations), $M > 2 \times M_{\text{res}}$. Error bars represent the Poissonian error in the counts.

(which allows only a single fragmentation within a time step), M_{res} cannot be chosen to be arbitrarily small, as in this case multiple fragmentation becomes improbable (i.e., $N_p \ll 1$) only if the time resolution (and hence the computational time) is extremely high. For instance, if we keep the ratio between M_{res} and the mass of the main halo in the tree fixed at the present-day value, the time for one Monte Carlo realization is longer by an order of magnitude. Since our aim is to track the merger hierarchy to very high redshifts, to keep the computational time down to acceptable values, we have approximated the fraction of accreted mass by the fitting formula

$$F_a = a[\log(M/M_{\text{res}})]^{-b}, \quad (6)$$

instead of integrating numerically the mass function of progenitors with $M < M_{\text{res}}$ at every branch of the tree. Here, depending on mass and redshift, a and b are in the range $(0.3\text{--}40) \times 10^{-3}$ and $0.3\text{--}0.8$, respectively, and have been adjusted empirically to provide a fit to equation (4) within 5% in the range of masses and redshifts considered. Beside conserving mass, a merger tree algorithm must reproduce at all redshifts the conditional mass function predicted by the EPS theory. The comparison is shown in Figures 1 and 2; for this set of realizations we have used 820 time steps logarithmically spaced in expansion factor between $z = 0$ and $z = 20$. With the above prescriptions, the tree typically agrees with the EPS predictions within a factor of 2 up to $z = 20$ for masses greater than $3 \times M_{\text{res}}$. Each realization that we generate tracks backward the merger history of 220 parent halos at the present epoch picked over the mass range $10^{11} M_{\odot} < M_0 < 10^{15} M_{\odot}$, where the lower limit has

been chosen to match the minimum mass effectively probed by dynamical studies of SMBH hosts in the local universe.

These are broken up into as many as 70,000 progenitors by $z = 20$. One issue of concerns involves systematic deviations of the unconditional (and conditional) Press-Schechter (PS) mass function compared to N -body simulations. At low redshifts, the PS mass function overpredicts the number of small halos by a factor of 1.5–2 (e.g., Gross et al. 1998; Sheth & Tormen 1999). The model and simulation results agree well on all scales at $z \sim 1$, while at higher redshifts the abundance of large-mass halos is underestimated by the PS model (Somerville et al. 2000). In general, halo merging histories constructed using the EPS formalism are reasonably consistent with those extracted from N -body simulations. At very high redshift ($z \gtrsim 10$), a recent cosmological simulation by Jang-Condell & Hernquist (2001) finds good agreement with the PS mass function for the lowest halo masses of interest here.

3. GROWTH OF SUPERMASSIVE BLACK HOLES

3.1. Pregalactic Seeds

Following MR01, we assume that one seed BH forms in each of the rare density peaks above $\nu\sigma$ at $z = 20$. All seed BHs are assigned a mass $m_{\bullet} = 150 M_{\odot}$. In general, we find that our results are not very sensitive to the precise mass choice for these seed holes (see § 4). As our fiducial model we take $\nu = 3.5$, corresponding in the assumed Λ CDM cosmology to minihalos of mass $M_{\text{seed}} = 1.1 \times 10^7 h^{-1} M_{\odot}$. This is larger than the minimum mass threshold for bar-

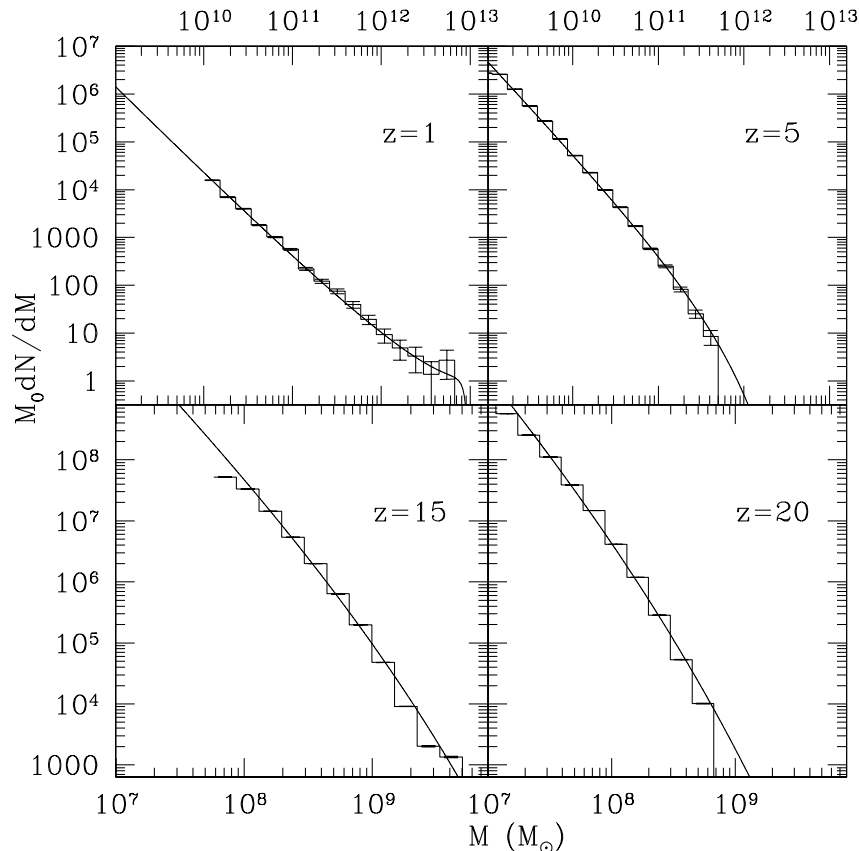


FIG. 2.—Same as Fig. 1, but for $z_0 = 0$, $M_0 = 4 \times 10^{13} M_{\odot}$ parent halo

ionic condensation, $M_{\min} \approx 5 \times 10^5 M_{\odot}$ ($h = 0.65$), found in the numerical simulations of Fuller & Couchman (2000). Above M_{\min} the H_2 cooling time is shorter than the Hubble time at virialization, the gas in the central halo regions becomes self-gravitating, and stars can form. We notice that the EPS formalism predicts on the order of 1 progenitor above M_{seed} for our lower mass parent halo, $M_0 = 10^{11} M_{\odot}$. Also, our resolution mass, $M_{\text{res}} = 10^{-3} M_0 (1+z)^{-3.5}$ is always lower at $z = 20$ than M_{seed} for all parent halos with masses $M_0 < 10^{15} M_{\odot}$.

A pregalactic halo at $z = 20$ is characterized by a virial radius (defined as the radius of the sphere encompassing a mean mass density $\Delta_{\text{vir}} \rho_{\text{crit}}$, where ρ_{crit} is the critical density for closure at the redshift z and Δ_{vir} is the density contrast at virialization)⁴ $r_{\text{vir}} = 390 \text{ pc } M_7^{1/3} h^{-1}$, and a circular velocity $V_c = 10.5 \text{ km s}^{-1} M_7^{1/3}$ at r_{vir} . The gas collapsing along with the dark matter perturbation will be shock-heated to the virial temperature $T_{\text{vir}} \approx 3200 \text{ K } M_7^{2/3}$, where M_7 is the halo mass in units of $10^7 h^{-1} M_{\odot}$. The total baryonic mass within the virial radius is equal to $(M_{\text{seed}} \Omega_b / \Omega_0)$. In a Gaussian theory, halos more massive than the ν - σ peaks contain a complementary error fraction $\text{erfc}(\nu/\sqrt{2}) (= 0.00047$ for $\nu = 3.5$) of the mass of the universe. Therefore, the mass density parameter of our “3.5 σ ” pregalactic holes is

$$\Omega_{\bullet} = \frac{0.00047 \Omega_0 m_{\bullet}}{1.1 \times 10^7 h^{-1} M_{\odot}} \gtrsim 2 \times 10^{-9} h. \quad (7)$$

This is much smaller than the density parameter of the supermassive variety found in the nuclei of most nearby galaxies,

$$\Omega_{\text{SMBH}} = \frac{6 \times 10^5 h M_{\odot} \text{ Mpc}^{-3}}{2.8 \times 10^{11} h^2 M_{\odot} \text{ Mpc}^{-3}} \approx 2 \times 10^{-6} h^{-1}, \quad (8)$$

where the value at the denominator is the critical density today, and we have taken for the local density of SMBHs the value recently inferred by Merritt & Ferrarese (2001). Clearly, if SMBHs form out of very rare Population III BHs, the present-day mass density of SMBHs must have been accumulated during cosmic history via gas accretion, with BH-BH mergers playing a secondary role. This is increasingly less true, of course, if the seed holes are more numerous and populate the 2 or 3 σ peaks instead, or halos with smaller masses at $z > 20$ (MR01).

The choice of where to initially locate our seed BHs, while motivated by recent numerical simulations of the formation of the first stars, is clearly somewhat arbitrary. Computational costs do not allow us to follow the merger hierarchy much beyond $z = 20$, or down to minihalo masses smaller than M_{seed} . As argued by MR01, if an extreme IMF is linked to primordial H_2 chemistry and cooling, it seems unlikely that the formation of massive BHs from zero-metallicity VMSs might have been a very efficient process, since metal-free VMSs are copious sources of Lyman-Werner photons (Bromm, Kudritzki, & Loeb 2001). This radiation may photodissociate H_2 elsewhere within the host halo, escape into the intergalactic medium (IGM) and form a soft UV background that suppresses molecular cooling throughout the universe (Haiman, Abel, & Rees 2000), and inhibit the formation of a much more numerous population of VMSs. Moreover, VMSs in the mass range $140 M_{\odot} \leq m_{\star}$

$\leq 260 M_{\odot}$ are predicted to make pair-instability supernovae with explosion (kinetic) energies of up to 10^{53} ergs. This is typically much larger than the baryon binding energy of a subgalactic fragment, $E_b \approx 10^{52.5} \text{ ergs } h^{-1} \Omega_b \times M_7^{5/3} [(1+z)/20]$. Minihalos will then be completely disrupted (“blown away”) by such energetic events, and metal-enriched material will be returned to the IGM (e.g., Madau, Ferrara, & Rees 2001) and later collect in the cores of more massive halos formed by subsequent mergers, where a “second” generation of stars may now be able to form with an IMF that is less biased toward very high stellar masses (Schneider et al. 2002).

3.2. Major Mergers

We model each dark halo as a singular isothermal sphere (SIS) with circular velocity V_c , one-dimensional velocity dispersion $\sigma_{\text{DM}} = V_c/\sqrt{2}$, and density $\rho(r) = V_c^2/4\pi G r^2$, truncated at the virial radius. When two halos of mass M and M_s merge, the “satellite” (less massive) progenitor (mass M_s) is assumed to sink to the center of the more massive pre-existing system on the Chandrasekhar dynamical friction (against the dark matter background) timescale

$$t_{\text{df}} = 1.17 \frac{r_{\text{circ}}^2 V_c}{G M_s \ln \Lambda} \epsilon^{\alpha} = 1.65 \frac{1+P}{P} \frac{1}{H \sqrt{\Delta_{\text{vir}} \ln \Lambda}} \Theta \quad (9)$$

(Lacey & Cole 1993; Binney & Tremaine 1987), where V_c is the circular velocity of the satellite in the new halo of mass $M + M_s$ and virial radius r_{vir} , r_{circ} is the radius of the circular orbit having the same energy as the actual orbit, the “circularity” ϵ is the ratio between the orbital angular momentum and that of the circular orbit having the same energy, H is the Hubble parameter, $P = M_s/M$ is the (total) mass ratio of the progenitors, and the Coulomb logarithm is taken to be $\ln \Lambda \approx \ln(1+P)$. The dependence of this timescale on the orbital parameters is contained in the term

$$\Theta = \epsilon^{\alpha} (r_{\text{circ}}/r_{\text{vir}})^2. \quad (10)$$

The most likely orbits occurring in cosmological CDM simulations of structure formation have circularity $\epsilon = 0.5$ and $r_{\text{circ}}/r_{\text{vir}} = 0.6$ (e.g., Tormen 1997; Ghigna et al. 1998). With these initial orbital parameters, recent numerical investigations by van den Bosch et al. (1999) and Colpi, Mayer, & Governato (1999) suggest a value $\alpha = 0.4$ – 0.5 for the exponent in equation (10). Here we assume $\Theta = 0.3$, but we note that the merger timescale computed in this way does not include the increase in the orbital decay timescale due to tidal stripping of the satellite (Colpi et al. 1999). Satellites will merge with the central galaxy on timescales shorter than the then Hubble time only in the case of major mergers, $P \gtrsim 0.3$. In minor mergers, tidal stripping may leave the satellite BH almost “naked” of its dark halo, too far from the center of the remnant for the formation of a BH binary.

Figure 3 shows the number of major mergers per unit redshift bin experienced by halos of different masses. For galaxy-sized halos, this quantity happens to peak in the redshift range 2–4, the epoch when the observed space density of optically selected quasars also reaches a maximum. Hydrodynamic simulations of major mergers have shown that a significant fraction of the gas in interacting galaxies falls to the center of the merged system (Mihos & Hernquist 1994, 1996); the cold gas may eventually be driven into the very inner regions, fueling an accretion episode and the

⁴ For the assumed cosmology this can be approximated by $\Delta_{\text{vir}} = 178 \Omega^{0.45}$ (Eke, Navarro, & Frenk 1998).

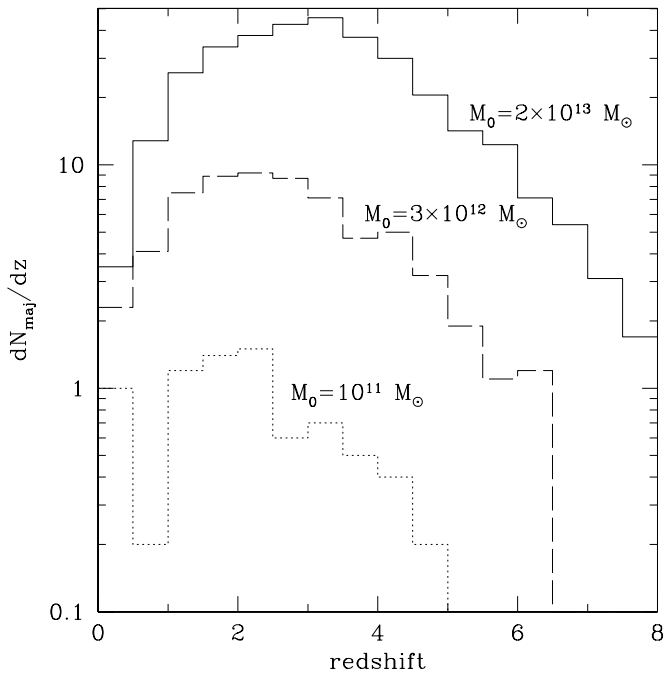


FIG. 3.—Mean number of major mergers experienced per unit redshift by halos with masses greater than $10^{10} M_{\odot}$. Progenitors of an $M_0 = 2 \times 10^{13} M_{\odot}$ halo (solid line), $M_0 = 3 \times 10^{12} M_{\odot}$ halo (dashed line), and $M_0 = 10^{11} M_{\odot}$ halo (dotted line) at $z = 0$.

growth of the nuclear BH. In the following we shall make the simplifying assumption that SMBHs accrete material only during major mergers.

3.3. Accretion History

The physical processes that determine the amount of accreted gas and the characteristic accretion timescales onto SMBHs are poorly understood, and different prescriptions have been proposed in the literature to explain the observed evolution of quasi-stellar objects (QSOs) within hierarchical clustering cosmologies. We shall not attempt here to model these processes in detail, but we note that the fraction of cold gas ending up in the hole must depend on the properties of the host halo in such a way as to ultimately lead to the observed correlation between stellar velocity dispersion and SMBH mass. Using the most up-to-date set of BH mass measurements, Ferrarese (2002) finds

$$m_{\text{BH}} = (4.4 \pm 0.9) \times 10^7 M_{\odot} \sigma_{c,150}^{4.58 \pm 0.52}, \quad (11)$$

where $\sigma_{c,150}$ is the bulge velocity dispersion (defined within an aperture of size $\lesssim 0.5$ kpc) in units of 150 km s^{-1} . Gebhardt et al. (2000) and Tremaine et al. (2002) report a similar relation with a somewhat shallower slope. From a sample of spirals and elliptical galaxies with $\sigma_c > 70 \text{ km s}^{-1}$, Ferrarese (2002) also shows that the stellar velocity dispersion is strictly correlated with the asymptotic value of the circular velocity V_c measured well beyond the optical radius,

$$\log V_c = (0.88 \pm 0.17) \log \sigma_c + (0.47 \pm 0.35). \quad (12)$$

To avoid introducing additional parameters to our model, as well as uncertainties linked to gas cooling, star formation, and supernova feedback, we combine the two previous relations and adopt the following simple prescription for the

mass accreted by an SMBH during each major merger:

$$\Delta m_{\text{acc}} = 1.3 \times 10^4 M_{\odot} \mathcal{H} V_{c,150}^{5.2}, \quad (13)$$

where $V_{c,150}$ is the circular velocity of the merged system in units of 150 km s^{-1} (cf. Kauffmann & Haehnelt 2000). We assume this mass is accreted by the BH in the more massive progenitor halo at the Eddington rate, after about a dynamical timescale (estimated at one-tenth the virial radius, $t_{\text{dyn}} = 0.1 r_{\text{vir}} / V_c$). The normalization factor \mathcal{H} is on the order of unity and is fixed in order to reproduce the $m_{\text{BH}}-\sigma_c$ relation observed locally.

The above relations are only valid up to a value of the velocity dispersion corresponding to galaxy group and cluster scales. For instance, the SMBH in M87 has a mass of $m_{\text{BH}} = 3 \times 10^9 M_{\odot}$ (Harms et al. 1994), perfectly correlating with the observed circular velocity $V_c = 506 \text{ km s}^{-1}$ of the galaxy, but not with the circular velocity of the Virgo Cluster ($V_c \approx 1000 \text{ km s}^{-1}$). Moreover, the larger halo ($V_c = 1280 \text{ km s}^{-1}$) considered in our merger-tree set would contain at $z = 0$ an SMBH more massive than $10^{10} M_{\odot}$; this would lead to an overestimate of the quasar LF at late epochs. Following Kauffmann & Haehnelt (2000), we have then inhibited gas accretion onto SMBHs in all halos with $V_c > 600 \text{ km s}^{-1}$. We find that this assumption affects only the accretion history of the SMBHs hosted in the two more massive halos of our realizations, and only at late epochs. On small mass scales, on the other hand, accretion onto BHs hosted by minihalos with virial temperature $T_{\text{vir}} < 10^4 \text{ K}$ may be inhibited by UV radiation. Photoionization by an internal UV source or a nearby external one will heat the gas inside these shallow potential wells to 10^4 K , leading to the photoevaporation of baryons out of their hosts. After the reionization epoch, gas cooling, star formation, and accretion onto BHs may only be possible within more massive halos with virial temperatures $T_{\text{vir}} \gtrsim \text{a few} \times 10^4 \text{ K}$, where pressure support is reduced and gas can condense because of atomic line processes. Therefore, in our model we suppress gas accretion onto all BHs in minihalos with $T_{\text{vir}} < 10^4$. We have checked that this assumption has little or no effect at $z \lesssim 10$.

Modeling gas accretion onto BHs with the recipes just described, we find that, along cosmic history, most of the final mass of SMBHs come from gas accretion, rather than from BH merging. The final mass m of the SMBH formed after coalescence assumes the entropy-area relation for BHs (maximally efficient radiative merging; e.g., Ciotti & van Albada 2001); the total entropy S of the system remains unchanged, $S = m^2/4 = S_1 + S_2 = m_1^2/4 + m_2^2/4$ (taking $G = c = k = h = 1$; Hawking & Ellis 1973). In contrast with previous work (e.g., Kauffmann & Haehnelt 2000; Menou et al. 2001), we do not make the simplifying assumption that the two preexisting holes coalesce instantaneously. The evolution of SMBH pairs will be discussed in the next section.

3.4. Dynamical Evolution of BH Binaries

In our model, the merging—driven by dynamical friction against the dark matter background—of two halo+BH systems with mass ratio $P \gtrsim 0.3$ will drag in a satellite BH toward the center of the more massive progenitor; this will inevitably lead to the formation of a bound SMBH binary in the violently relaxed core of the newly merged stellar system. Figure 4 shows the typical mass ratio of binary BHs together with the mean mass of the larger member of the

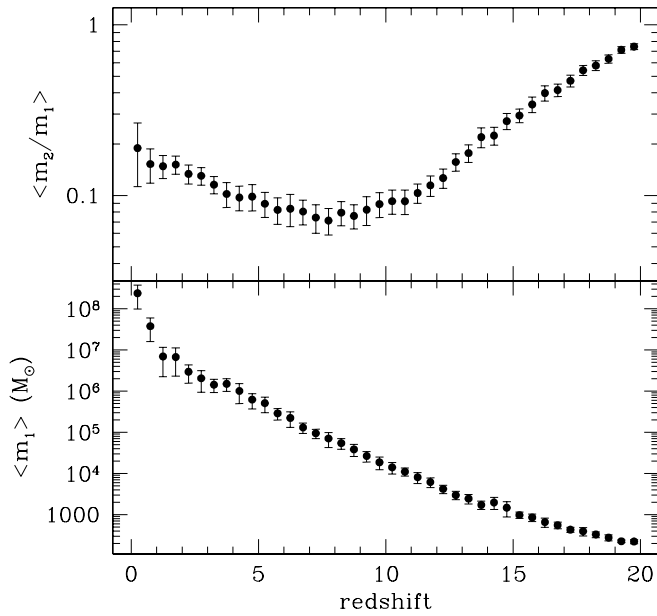


FIG. 4.—Mass ratio of BH binaries (*upper panel*) and mass of the larger BH (*lower panel*) are shown as a function of redshift. The points show the mean values and 1σ error bars from all Monte Carlo realizations. At high redshift, binary members are seed Population III BHs with nearly equal masses; as time goes on the holes grow mainly because of gas accretion, and low mass ratios become more probable.

pair as a function of redshift. At late epochs, most of the BH pairs have unequal masses and, since the growth history of SMBHs does not track that of dark matter halos, a major merger between halos does not necessarily result in a BH binary with a large P , as evident from the upper panel of the figure.

The subsequent evolution of BH binaries was first outlined by Begelman, Blandford, & Rees (1980). Consider a binary with BH masses $m_1 \geq m_2$ and semimajor axis $a(t)$ in an isotropic background of stars of mass $m_* \ll m_2$ and density $\rho_*(r)$. We use a simple model for the initial central stellar distribution, an SIS with a velocity dispersion comparable to the halo σ_{DM} ,

$$\rho_* = \frac{\sigma_{\text{DM}}^2}{2\pi Gr^2}. \quad (14)$$

This appears to be a good assumption for early-type lens galaxies (e.g., Koopmans & Treu 2003). When the age of the system is larger than the stellar relaxation time, the equilibrium distribution of stars around a BH is expected to be cuspy, $\rho_* \propto r^{-7/4}$, within the gravitational sphere of influence of the BH, even if the original profile had a core (Bahcall & Wolf 1976).

The binary forms at a separation $a_b = G(m_1 + m_2)/(2\sigma_{\text{DM}}^2)$, at which the enclosed stellar mass equals $m_1 + m_2$, and initially hardens by dynamical friction from distant stars acting on each BH individually. But as the binary separation shrinks (the binary “hardens”), the effectiveness of dynamical friction slowly declines because distant encounters perturb only the binary’s center of mass but not its semimajor axis. The BH pair then hardens via three-body interactions, i.e., by capturing the stars that pass within a distance $\sim a$ of it and ejecting them (“gravitational slingshot”) at much higher velocities, $v_{\text{ej}} \approx V_{\text{bin}} \equiv [G(m_1 + m_2)/a]^{1/2}$, where V_{bin} is the relative velocity of the

two BHs if their orbit is circular: this is the hard binary stage. In Quinlan’s (1996) simulations of the dynamical evolution of massive BH binaries, the system does not become hard until the value of a falls below

$$a_h = \frac{Gm_2}{4\sigma_{\text{DM}}^2} = 1 \text{ pc} \left(\frac{m_2}{10^{7.3} M_\odot} \right) \sigma_{\text{DM},150}^{-2} \quad (15)$$

(Quinlan 1996).⁵ We assume that the “bottleneck” stages of the binary shrinking occur for separations $a < a_h$; in a major merger, after a dynamical friction timescale, we form the BH binary at a separation a_h and let it evolve.

In a fixed background, the hardening timescale $|a/\dot{a}|$ decreases with the value of a ,

$$t_h = \frac{\sigma_{\text{DM}}}{G\rho_* a H} = 10^{3.4} \text{ yr} \left(\frac{a}{\text{pc}} \right) \left(\frac{15}{H} \right) \sigma_{\text{DM},150}^{-1}, \quad (16)$$

and the binary would spend the longest period of time with $a \approx a_h$. Here the second equality assumes an SIS (eq. [14]) down to a distance a from the center, and the dimensionless hardening rate is $H \approx 15$ in the limit of a very hard, equal-mass binary (Quinlan 1996). If the hardening continues sufficiently far, gravitational radiation losses can take over, and the two BHs rapidly coalesce on the timescale (for a circular orbit)

$$t_{\text{gr}} = \frac{5c^5 a^4(t)}{256 G^3 m_1 m_2 (m_1 + m_2)} \quad (17)$$

(Peters 1964).

If the binary can shrink to a separation

$$a_{\text{gr}} = 0.014 \text{ pc} \left[\frac{(m_1 + m_2)m_1 m_2}{10^{21.3} M_\odot^3} \right]^{1/4}, \quad (18)$$

then the binary will coalesce within 10 Gyr because of the emission of gravitational waves. Here we have normalized to the case $m_1 = m_2 = 10^7 M_\odot$. In our model we neglect the recoil due to the nonzero net linear momentum carried away by gravitational waves in the coalescence of two unequal mass BHs (“gravitational rocket”). Radiation recoil is a strong-field gravitational effect that depends on the lack of symmetry in the system and may eject massive BHs from galaxy cores. To date, the outcome of a gravitational rocket remains uncertain. Newtonian approximation and perturbative calculations of two orbiting Schwarzschild holes suggest maximum recoil velocities on the order of 70–100 km s^{−1} (Fitchett 1983, Fitchett & Detweiler 1984).

In practice, however, one cannot assume a fixed stellar background in estimating the rate of BH mergers, as the hardening of the binary modifies the stellar density ρ_* in equation (16); the shrinking of the pair removes mass interior to the binary orbit, depleting the galaxy core of stars and slowing down further hardening. The effect of loss-cone depletion (the depletion of low angular momentum stars that get close enough to extract energy from a hard binary) is one of the major uncertainties in computing the merger time and makes it difficult to construct viable merger scenarios for BH binaries. A recent analysis by Yu (2002) has

⁵ The standard definition of a “hard” binary, one where its binding energy $E_b = Gm_1 m_2/a$ exceeds the typical kinetic energy of the surrounding stars $3m_*\sigma_{\text{DM}}^2/2$ (Binney & Tremaine 1987), is inapplicable to massive BH binaries as they are always hard if bound. Quinlan (1996) defines hardness instead in terms of the binary orbital velocity; in his definition a hard binary hardens at a constant rate.

shown that in significantly flattened or triaxial galaxies the supply of low-angular momentum stars may be sufficient to reach a_{gr} . A massive gaseous disk surrounding the binary may further speed up the merger rate (Gould & Rix 2000). N -body simulations of BH binary decay suggest that the wandering of the binary center of mass from the galaxy center (and to a lesser extent the diffusion of stars into the loss cone) may also work to mitigate the problems associated with loss-cone depletion (which may ultimately cause the binary to “stall”) and helps the binary merge (Quinlan & Hernquist 1997; Milosavljevic & Merritt 2001). Here we adopt a simple analytical scheme following Merritt (2000) that qualitatively reproduces the evolution observed in N -body simulations. If M_{ej} is the stellar mass ejected by the BH pair, the binary evolution and its effect on the galaxy core are determined by the coupled equations

$$\frac{d}{dt} \left(\frac{1}{a} \right) = H \frac{G \rho_*}{\sigma_{\text{DM}}}, \quad (19)$$

$$\frac{dM_{\text{ej}}}{d \ln(1/a)} = J(m_1 + m_2), \quad (20)$$

where J is the dimensionless mass ejection rate, $J \approx 1$ nearly independent of a for $a \ll a_h$ (Quinlan 1996). Integrating the second equation one finds $M_{\text{ej}} \approx J(m_1 + m_2) \ln(a_h/a)$; the binary ejects on the order of its own mass in shrinking from a_h to $a_h/3$. We assume that the stellar mass removal creates a core of radius r_c and constant density $\rho_c \equiv \rho_*(r_c)$, so that the ejected mass can be written as

$$M_{\text{ej}} = \frac{2\sigma_{\text{DM}}^2 r_c}{G} - \frac{4\pi}{3} \rho_c r_c^3 = \frac{4}{3} \frac{\sigma_{\text{DM}}^2 r_c}{G} \quad (21)$$

(Merritt 2000). From equations (20) and (21) one derives

$$r_c(t) = \frac{3}{4\sigma_{\text{DM}}^2} GJ(m_1 + m_2) \ln(a_h/a), \quad (22)$$

and the core density decreases as

$$\rho_c(t) = \frac{8\sigma_{\text{DM}}^6}{9\pi G^3 M_{\text{ej}}^2(t)}. \quad (23)$$

The above relations, assuming a constant σ_{DM} during the hardening of the binary, are strictly valid only if the stellar relaxation timescale is long compared to the hardening time. The binary separation quickly falls below r_c , and subsequent evolution is slowed down because of the declining stellar density, with a hardening time

$$t_h = \frac{2\pi r_c^2}{H \sigma_{\text{DM}} a}, \quad (24)$$

which now becomes increasingly long as the binary shrinks. In this model the mass ejected increases logarithmically with time, and the binary can “heat” background stars at radii r , $a \ll r \lesssim r_c$. In N -body simulations this may happen because of the Brownian motion of the binary induced by continuous interactions with other stars. Also, stars on eccentric orbits are most likely to interact with the binary and be removed, then lose their kinetic energy to the background as they spiral back in and are kicked out again.

Figure 5 shows the evolution of a binary of seed, intermediate-mass BHs in two dark matter halos with different velocity dispersion. The binary separation a shrinks as the

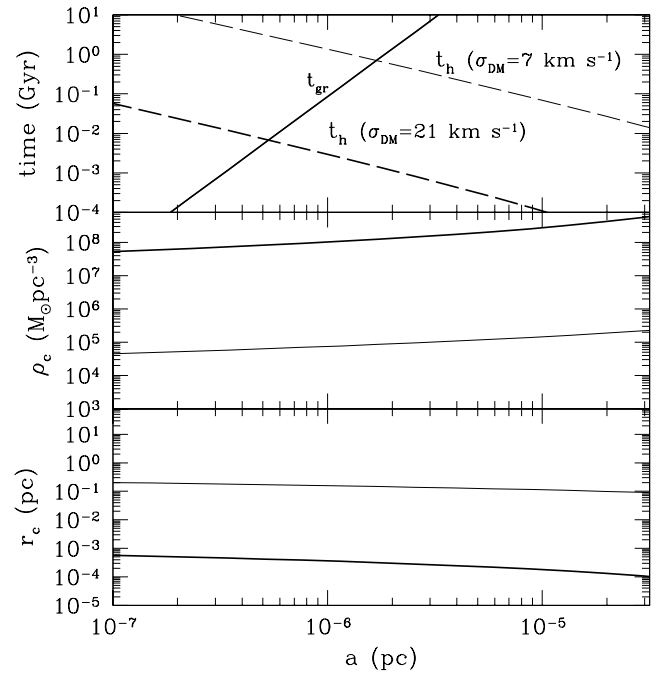


FIG. 5.—Evolution (from bottom to top) of core radius, core stellar density, and hardening timescale during the shrinking of a Population III BH binary against its separation. As the pair of $m_* = 150 M_\odot$ BHs shrinks, the initial $\rho_* \propto r^{-2}$ stellar cusp is gradually converted into a constant density core by the gravitational slingshot, and the hardening timescale lengthens. Thin lines: $\sigma_{\text{DM}} = 7 \text{ km s}^{-1}$. The total stellar mass ejected prior to coalescence is $7.5(m_1 + m_2)$. Thick lines: $\sigma_{\text{DM}} = 21 \text{ km s}^{-1}$. The total stellar mass ejected prior to coalescence is $6.5(m_1 + m_2)$.

pair interacts with the surrounding stellar field, and at the same time the ejection of stars decreases the central density creating a stellar core.

Finally, as it is conceivable that major mergers between galaxies may trigger bursts of star formation (e.g., Somerville, Primack, & Faber 2001), we further assume that a stellar cusp proportional to r^{-2} is promptly regenerated after every major merger event, replenishing the mass displaced by the BH binary. For a fixed binary mass the coalescence timescale is shorter in the case of more massive galaxies. The evolution of two SMBH binaries in a $\sigma_{\text{DM}} = 200 \text{ km s}^{-1}$ halo is depicted in Figure 6.

An equal mass binary with $m_1 = m_2 = 10^7 M_\odot$ needs a longer time to merge than a binary with $m_1 = 10^7 M_\odot \gg m_2$, as it must eject a larger number of stars. A comparison with a straightforward extrapolation of Milosavljevic & Merritt (2001) N -body results shows that the scheme we adopt tends to overestimate the binary evolution timescale by about a factor of 3 (scaling to real galaxies like M32 and M87). Two main factors contribute to this discrepancy: first, Milosavljevic & Merritt (2001) let the slope of the density profile change smoothly during the hardening of the binary, ending with a shallow cusp proportional to r^{-1} rather than with a flat core; second, they take into account the Brownian motion of the binary, which makes the BHs interact with a larger number of stars in the central region. Nevertheless, the coalescence timescales estimated in our model may be too short, since it is the total stellar density that is allowed to decrease following equation (23), not the density of low angular momentum stars (i.e., we neglect the depopulation of the loss cone); furthermore, our model assumes replenishment of the stellar cusp after every major merger. Yu (2002)

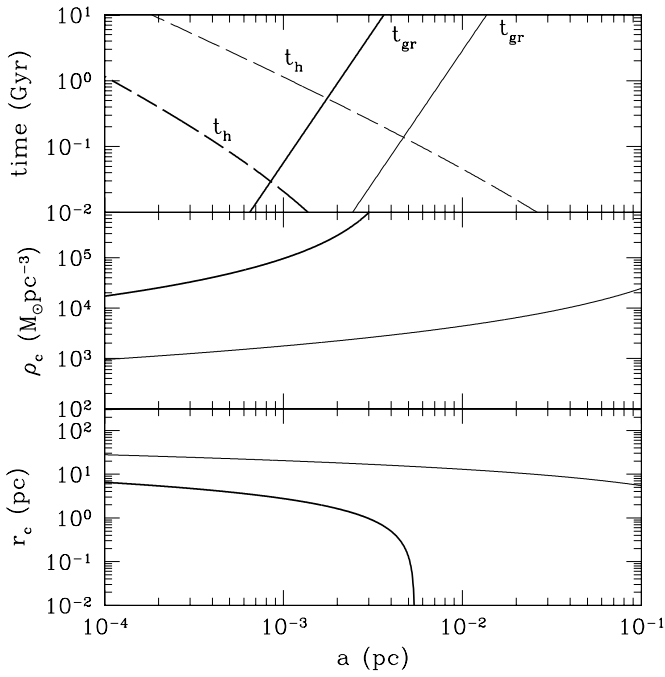


FIG. 6.—Same as Fig. 5, but for an SMBH binary in a halo with $\sigma_{\text{DM}} = 140 \text{ km s}^{-1}$. *Thin lines:* $m_1 = m_2 = 10^7 M_\odot$. The total stellar mass ejected prior to coalescence is $5(m_1 + m_2)$. *Thick lines:* $m_1 = 10^7 M_\odot$, $m_2 = 10^5 M_\odot$. The total stellar mass ejected prior to coalescence is $2(m_1 + m_2)$.

has recently studied the merger of binary SMBHs assuming the central stellar profiles observed by Faber et al. (1997) in a sample of local galaxies and finds that BH coalescence timescales may in some case be longer than the Hubble time.

3.5. Triple BH Interactions

The dynamical evolution of SMBH binaries may be disturbed by a third, incoming BH if another major merger takes place before the preexisting binary has had time to coalesce (e.g., Hut & Rees 1992; Xu & Ostriker 1994). In a minor merger, the intruder BH is stripped of most of the surrounding dark and luminous matter; the ensuing long dynamical friction timescale does not allow a close encounter between the central binary and the intruder. Within our scheme, these BHs remain wandering in galaxy halos through successive mergers. If the incoming hole reaches the sphere of influence (determined in our model by the hardening distance a_h) of the central binary, the three BHs are likely to undergo a complicated resonance-scattering interaction, leading to the final expulsion of one of the three bodies (gravitational slingshot). Typically, an encounter between an intruder of mass m_{int} smaller than both binary members leads to a scattering event, where the binary recoils by momentum conservation and the incoming lighter BH is ejected from the galaxy nucleus. The binary also becomes more tightly bound, each such encounter typically increasing its binding energy E_b by the amount $\langle \Delta E/E_b \rangle \approx 0.4 m_{\text{int}}/(m_1 + m_2)$ (Hills & Fullerton 1980; Colpi, Possenti, & Gualandris 2002). By contrast, when the intruder is more massive than one or both binary components, the probability of an exchange is extremely high: the incoming hole becomes the member of a new binary, and the lightest BH of

the original pair gets ejected (Hills & Fullerton 1980). For mass ratios $m_{\text{int}}/(m_1 + m_2) \lesssim 2$, most of the increase in the binding energy of the pair is because of the actual shrinking of the orbit, while above this value the binding energy rises mainly due to the replacement of a low-mass member by a more massive BH. In the latter case, and for head-on collisions and equal mass binaries, the fractional increase in binding energy is approximately constant with a value of 3.1 (Hills & Fullerton 1980).

If the binary is hard the kinetic energy and momentum of the intruder are much lower than the orbital binding energy and the recoil momentum of the ejected body (we have checked a posteriori that this is true in nearly all cases of triple interactions). Conservation of energy and momentum in the interaction then allows one to estimate the recoil velocity of the binary and intruder. Let m_{ej} be the mass of the lightest of the three BHs and m_{bin} the mass of the final binary; i.e., $m_{\text{ej}} = m_{\text{int}}$ and $m_{\text{bin}} = m_1 + m_2$ in a scattering event, $m_{\text{ej}} = m_2$ and $m_{\text{bin}} = m_{\text{int}} + m_1$ for exchanges. The kinetic energy of the ejected BH and of the binary after the encounter will then be

$$K_{\text{bin}} = \frac{\Delta E}{1 + (m_{\text{bin}}/m_{\text{ej}})}, \quad (25)$$

$$K_{\text{ej}} = \frac{\Delta E}{1 + (m_{\text{ej}}/m_{\text{bin}})}. \quad (26)$$

We adopt a simple scheme, in which the following apply:

1. If $m_{\text{int}} < m_2$, a scattering event occurs, with $\langle \Delta E/E_b \rangle = 0.4 m_{\text{int}}/(m_1 + m_2)$. The new semimajor axis is $a_1 = a_0/[1 + 0.4 m_{\text{int}}/(m_1 + m_2)]$.
2. If $m_2 < m_{\text{int}} < 2(m_1 + m_2)$, an exchange with $\langle \Delta E/E_b \rangle = 0.4 m_{\text{int}}/(m_1 + m_2)$ takes place. The new semimajor axis is $a_1 = a_0(m_{\text{int}}/m_2)[1 + 0.4 m_{\text{int}}/(m_1 + m_2)]$.
3. If $m_{\text{int}} > 2(m_1 + m_2)$, again an exchange happens, with $\langle \Delta E/E_b \rangle = 0.9$ (we have rescaled the value of 3.1 given by Hills & Fullerton 1980 for head-on collisions to account for a distribution of impact parameters). The new semimajor axis is $a_1 = 0.53 a_0(m_{\text{int}}/m_2)$.

In all cases we have used equations (25) and (26) to estimate the recoil velocities. All triple interactions are followed along the merger tree, as they modify the binary separation during each encounter. At high redshift we find that the increase in binding energy causes the binary to shrink to a separation small enough that coalescence by gravitational radiation occurs, since most of these encounters happen among approximately equal-mass systems. At later epochs, events with low $m_{\text{int}}/(m_1 + m_2)$ mass ratios are more common (see Fig. 7), and the binding energy increases only slightly after such interactions.

What happens to a BH pair+intruder system after the slingshot mechanism? In an SIS+core halo, the gravitational potential is

$$\Phi(r) = -2\sigma_{\text{DM}}^2 \times \begin{cases} \frac{1}{2} + \ln \frac{r_{\text{vir}}}{r_c} - \frac{1}{6} \left(\frac{r}{r_c} \right)^2 & r < r_c, \\ 1 + \ln \frac{r_{\text{vir}}}{r} - \frac{2}{3} \frac{r_c}{r} & r_c < r < r_{\text{vir}}, \\ \frac{r_{\text{vir}}}{r} - \frac{2}{3} \frac{r_c}{r} & r > r_{\text{vir}}, \end{cases} \quad (27)$$

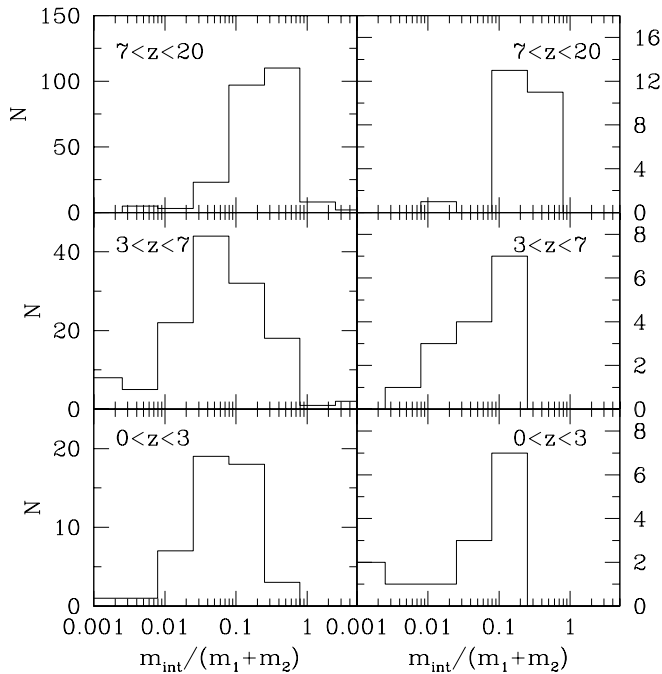


FIG. 7.—Number of triple interactions for different ratios between the intruder BH mass m_{int} and the mass $m_1 + m_2$ of the binary, in different redshift intervals. *Left:* $\sigma_{\text{DM}} = 250 \text{ km s}^{-1}$. *Right:* $\sigma_{\text{DM}} = 150 \text{ km s}^{-1}$. This histogram includes results from all 20 Monte Carlo realizations of the same halo mass. At very high redshift (*top panels*, $7 < z < 20$), equal mass system interactions are more common, while at low redshift (*bottom panels*, $0 < z < 3$), a high-mass binary typically interacts with an intruder of much lower mass. At intermediate-high redshift (*middle panels*, $3 < z < 7$), a transition regime occurs.

where the core radius r_c is that created by the hardening of the binary at the time of the triple interaction. If the kick velocity of the binary and/or single BH exceeds the escape speed $v_{\text{esc}} = (2|\phi|)^{1/2}$, the hole(s) will leave the galaxy altogether. We find that the recoil velocity of the single hole is larger than v_{esc} in 99% of encounters. The binary is ejected instead in only 8% of the encounters (Fig. 8) and typically at very high redshifts, when all BHs are in the same mass range.

For equal mass holes, both the binary and the single BH are ejected from radius r_{in} to infinity when the orbital velocity V_{bin} of the binary satisfies the condition

$$V_{\text{bin}} > 7.7 \sqrt{2\phi(r_{\text{in}})}. \quad (28)$$

The 1% of single BHs not escaping their host halos are typically slung to the periphery of the galaxy with, consequently, long dynamical friction timescales; most of the binaries recoil instead within the core and fall back to the center soon afterward, with $t_{\text{df}} < 0.01 \text{ Gyr}$. Since most of the ejected holes escape their hosts, in our scheme the number of *wandering* BHs due to the gravitational slingshot and retained within galaxy halos is thus significantly lower (by about a factor of 50) than that left over by minor mergers.

4. IMPLICATIONS

In this section we discuss some of the consequences predicted by our fiducial scenario (and a few variants) for the growth of SMBHs in the nuclei of galaxies.

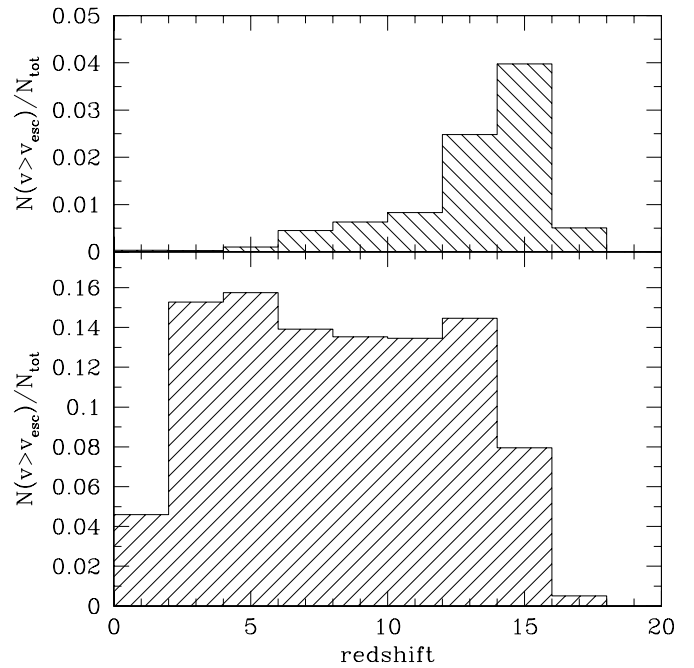


FIG. 8.—Fraction of BH binaries (*upper panel*) and single BHs (*lower panel*) with recoil velocity v larger than the escape speed, as a function of redshift. The histogram includes results from all Monte Carlo realizations.

4.1. The Quasars' Luminosity Function

In our framework, quasar activity is triggered by major mergers, and SMBHs accrete at the Eddington rate, $\dot{m}_{\text{E}} = 4\pi G m_p m_{\text{BH}} / (c \sigma_T \epsilon)$, where ϵ is the radiation efficiency. Accretion starts after about one dynamical timescale and lasts until a mass given by equation (13) has been added to the hole. Rest mass is converted to radiation with a 10% efficiency; only a fraction $f_B = 0.08$ of the bolometric power is radiated in the blue band. We have compared theoretical LFs at different redshifts with the most recent determination of the quasar blue LF from the Two-Degree Field (2dF) Survey ($0.3 < z < 2.3$; Boyle et al. 2000) and the SDSS ($3.3 < z < 5$; Fan et al. 2001a). The 2dF LF is a double power law, which we have extrapolated beyond redshift 2 assuming pure luminosity evolution; the best-fitting parameters for a Λ CDM cosmology are given by Boyle et al. (2000). The SDSS samples only the very bright end of the LF; Fan et al. (2001a) fitted a single power law to the data.

A detailed comparison at very early times required the use of ad hoc merger trees to simulate very luminous quasars in very massive, rare dark halos at high redshifts. For this purpose we have simulated the merging histories of $10^{15} M_{\odot}$ parent halos starting from $z = 3.5$ and applied the evolutionary scheme for their SMBHs outlined in the previous sections. As shown in Figure 9, our simple model reproduces reasonably well the observed LF of optically selected quasars in the redshift range $1 < z < 5$.

The slope at low luminosities matches the one inferred by Boyle et al. (2000) and is considerably flatter than the extrapolation of the SDSS power law. The tendency to overestimate the number of bright QSOs at $z \lesssim 1$ may be less severe because of the presence of a substantial population of (optically) obscured luminous AGNs at low redshifts suggested by recent *Chandra* results (e.g., Rosati et al. 2002; Barger et al. 2001), which may help reducing the discrepancy.

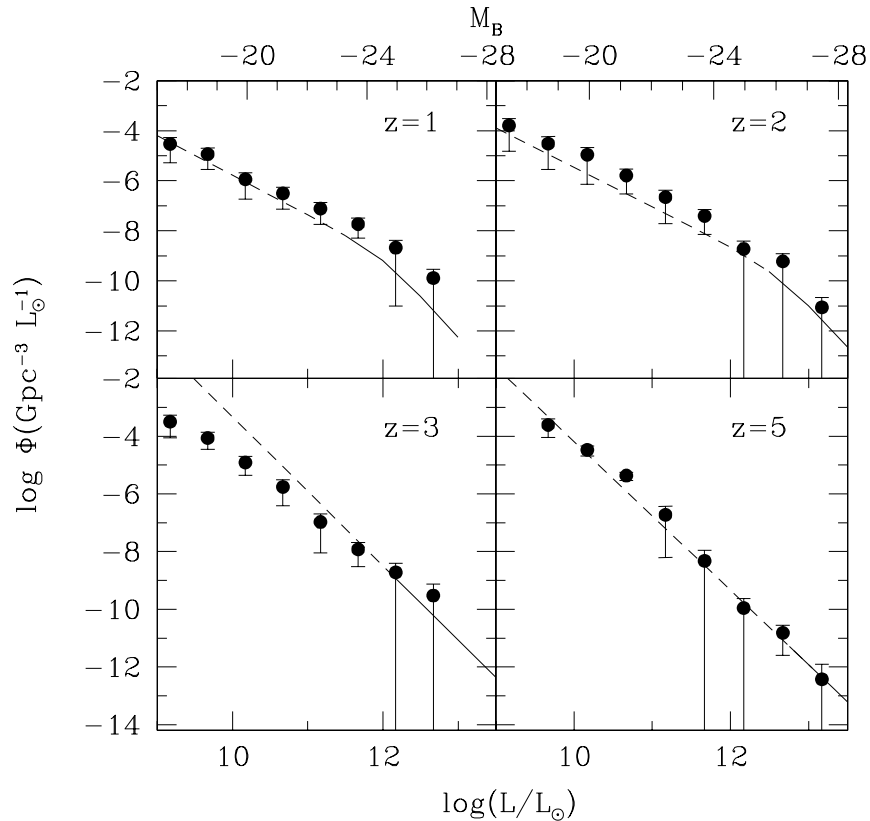


FIG. 9.—*B*-band LF of quasars at various redshifts. Filled circles represent the values predicted from our SMBH assembly and merging model history. Error bars indicate the poissonian error in the counts. Solid lines at $z = 1, 2$ are the 2dF LF, while solid lines at $z = 3, 5$ are the SDSS LF. The dashed lines show the extrapolation to faint magnitudes of the best-fit LF from Boyle et al. (2000; $z = 1, 2$) and Fan et al. (2001a; $z = 3, 5$).

To assess the impact on our results of making seed BHs more common or rarer, we have run realizations that place $m_{\bullet} = 150 M_{\odot}$ BHs at $z = 20$ in 3σ (lower bias) and 4σ (higher bias) peaks instead of the fiducial 3.5σ . We find that we can still reproduce the observed quasar LF by changing the major merger threshold from $P > 0.3$ in the lower bias case to $P > 0.1$ in the higher bias case. We have also run a case where the initial seed BH mass is $m_{\bullet} = 1000 M_{\odot}$ instead of $150 M_{\odot}$. We find little change at $z < 5$. However, the number of triple interactions at $z > 5$ increases; this is due to the fact that the hardening timescales are now longer, as more massive holes create larger core radii (see eqs. [23] and [24]). Overall, the number of BHs ejected in the IGM goes up by a factor of 2.

4.2. The $m_{\text{BH}}-\sigma_c$ Relation

In Figure 10 the local $m_{\text{BH}}-\sigma_c$ relation predicted by our scheme for the assembly history of SMBHs is compared to the fit given by Ferrarese (2002). The three curves in the lower corner show the $m_{\text{BH}}-\sigma_c$ relation we would obtain, assuming that when halos merge their BHs coalesce immediately, their masses sum directly, and there is no gas accretion. The slope is flatter and the normalization lower than observed. The steepening of the relation for initial seed BHs in higher σ peaks is a natural outcome of biasing. Assuming the entropy-area relation for the merging BHs tends instead to flatten the curves. The incapacity of mergers alone to yield the observed $m_{\text{BH}}-\sigma_c$ has been pointed out by Ciotti & van Albada (2001) using an argument based on the fundamental plane. The scatter in our model largely reflects the

time elapsed since the last major merger. While the final SMBH mass is set by the last episode of gas accretion and BH-BH coalescence, the host halo mass keeps growing through minor mergers and the accreting of small dark matter clumps with $M < M_{\text{res}}$. We find that lowering the threshold for major mergers has the effect of smoothing the mass assembly history of SMBHs, thus tightening the $m_{\text{BH}}-\sigma_c$ relation. Figure 11 illustrates the fact that the mass-growth history of SMBHs does not totally reflect that of their host halos and follows a more complex pattern, with a number of rapid accretion episodes.

The assembly history of two SMBHs is shown in Figure 12; one BH (labeled “1”) ends in a main, massive halo at the present epoch and the other (“2”) in a satellite at $z = 2.3$. The final mass of the two BHs is mostly due to gas accretion and does not depend on the initial conditions, i.e., whether the seed holes are hosted in the 3 or 3.5σ peaks. The number of major mergers between halos hosting SMBHs is larger in the 3σ peak case; only a fraction ends with the coalescence of the two holes before a triple BH interaction takes place, as gravitational slingshots are now more common. As an example, for a Milky Way-sized halo, the fraction of major mergers that ends up with the coalescence of the binary without a slingshot drops from 75% in the 3.5σ fiducial case to 30% for $\sigma = 3$.

4.3. Wandering BHs

It appears inevitable that significant numbers of triple BH interactions will take place at early times if the formation route for the assembly of SMBHs goes back to the very first

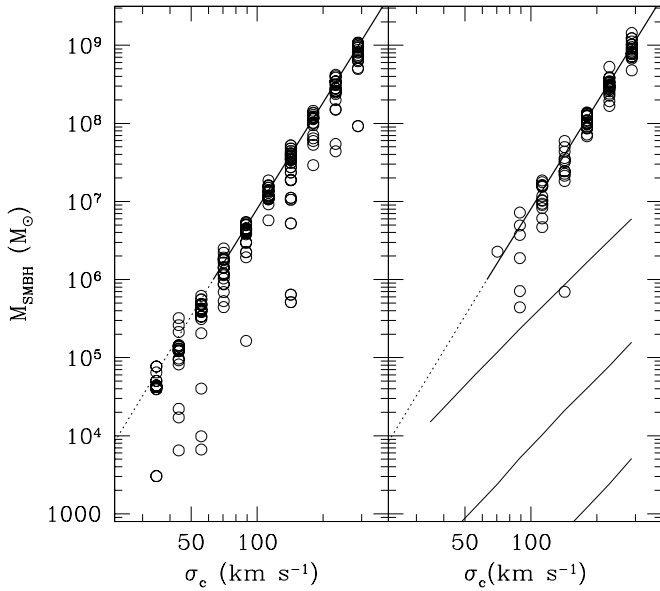


FIG. 10.—The $m_{\text{BH}}-\sigma_c$ relation at $z=0$. Every circle represents one nuclear BH in a halo of given σ_c . We started at $z=0$ with a discrete grid of halo masses (hence, with a discrete grid of σ_c ; see §§ 3.2 and 3.3) and performed several simulations for each mass. *Left*: Circles mark the results for our fiducial model with seed BHs in 3.5σ density peaks. The solid line shows Ferrarese’s (2002) best fit; its extrapolation to low σ_c -values is depicted by a dotted line. The holes deviating from the relation are hosted in galaxies that experienced their last major merger at $z > 1.5$. Since then, their host halos have grown due to minor mergers. *Right*: Same as the left panel, but for seed BHs in 4σ peaks. The three curves below (initial seed BHs in 3 , 3.5 , and 4σ peaks, from top to bottom, respectively) show the $m_{\text{BH}}-\sigma_c$ relation obtained assuming that when halos merge their BHs coalesce immediately, and there is no gas accretion. Note how the slope is flatter and the normalization lower than observed.

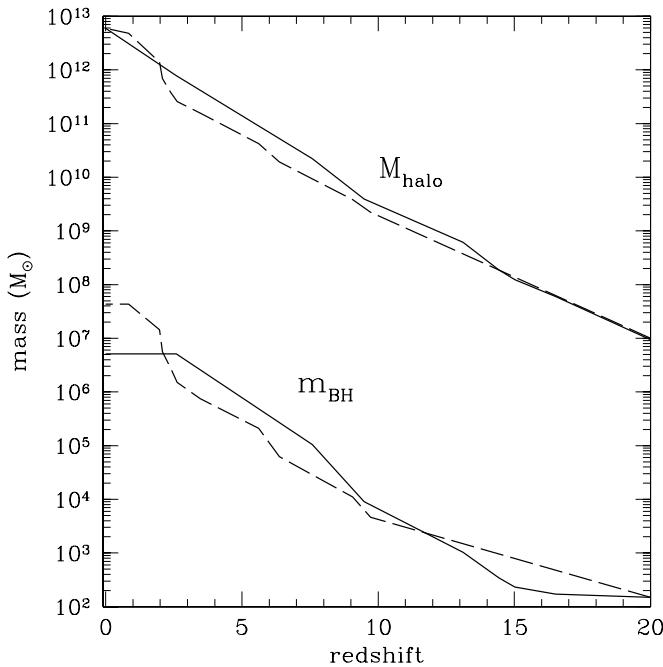


FIG. 11.—Two different realizations for the mass-assembly history of a galaxy halo with velocity dispersion $\sigma_{\text{DM}} = 160 \text{ km s}^{-1}$ at $z=0$ and its central SMBH. *Dashed line*: The halo experiences its last major merger at low redshift, and its hole follows the observed $m_{\text{BH}}-\sigma_c$ relation. *Solid line*: The halo has its final major merger at $z = 2.6$, when only a small fraction of its dark mass was already in place. The mass of its SMBH is only about 10% of that expected from the $m_{\text{BH}}-\sigma_c$ relation.

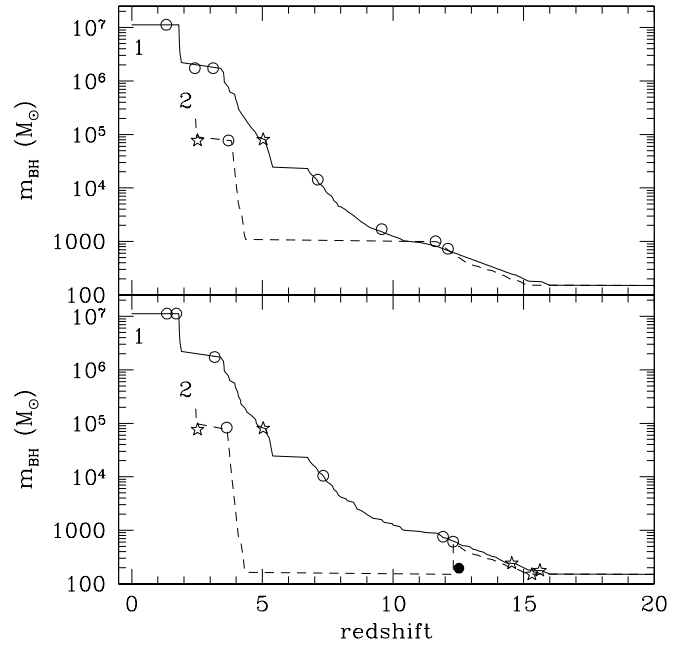


FIG. 12.—Mass-growth history of two SMBHs, one ending in a massive halo (“1”) with $\sigma_{\text{DM}} = 185 \text{ km s}^{-1}$ at $z=0$ and one in a satellite (“2”) with $\sigma_{\text{DM}} = 80 \text{ km s}^{-1}$ at $z = 2.3$. *Upper panel*: Seed holes in 3.5σ peaks at $z=20$. The BH mass grows after every major merger event due to gas accretion, independently of whether the other merging galaxy hosts another SMBH or not. The starred symbols mark the redshift of the major mergers of two parent halos both hosting an SMBH, but not ending up with the coalescence of the two SMBHs (indicated by stars). The circles mark the redshift when two SMBHs coalesce. Note how most of the mass of the lighter hole is gained in the most recent accretion episodes. *Lower panel*: Same as upper panel, but for seed BHs in 3σ peaks. The number of mergers not ending up with the coalescence of the two SMBHs (indicated by stars) is larger compared to the higher bias case. The black dot marks the rare event (occurring in the satellite galaxy) of a decrease of the central BH mass, caused by the ejection of the binary in a triple BH interaction.

generation of stars, and even more so if the seed holes are more numerous and populate the low- σ peaks. As discussed in § 3, our scheme predicts, along nuclear SMBHs hosted in galaxy bulges, a number of wandering BHs that are largely the result of minor mergers rather than of low-energy slingshots. In practice, for minor mergers, the dynamical friction timescale is longer than the Hubble time, and at $z=0$ the BHs are still on their way to the galactic center. Moreover, rare high-energy slingshots can eject the lighter holes out of the halo, giving origin to a population of free-floating “intergalactic BHs.” Even rarer events occur when the lighter BH and the binary are both ejected into the IGM.

The total mass in wandering BHs ranges from 1% to 10% of the mass of the central SMBH, for halos with $\sigma_{\text{DM}} = 50$ and 300 km s^{-1} , respectively. Figure 13 shows the mass function of wandering BHs at $z=0$ for two typical halos, $\sigma_{\text{DM}} = 100$ and 200 km s^{-1} , respectively.

In Figure 14 we show the total mass in BHs predicted by our scheme, and the relative contribution of nuclear, wandering and intergalactic BHs, as a function of redshift. At $z=0$ the mass in nuclear BHs is $\simeq 3.5 \times 10^5 M_\odot \text{ Mpc}^{-3}$, within 30% of the value given by Merritt & Ferrarese (2001), somewhat larger than the value estimated by Yu & Tremaine (2002) from SDSS data and similar to an early estimate by Salucci et al. (1999). The total mass is dominated by nuclear BHs at every epochs; however, at low redshifts, wandering BHs become increasingly more important.

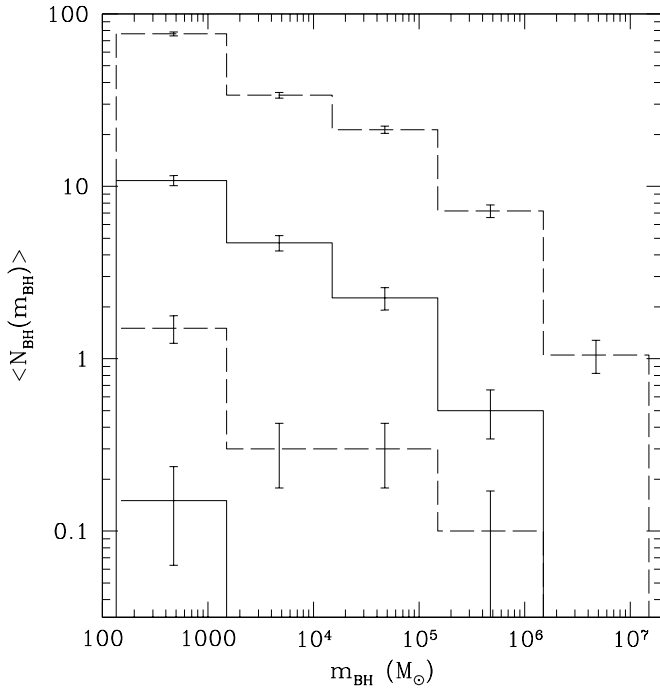


FIG. 13.—Mass function of wandering BHs at $z=0$, averaged over 20 Monte Carlo realizations of a galaxy-sized halo ($\sigma_{\text{DM}} = 100 \text{ km s}^{-1}$, solid lines), and 20 realizations of a more massive halo ($\sigma_{\text{DM}} = 200 \text{ km s}^{-1}$, dashed lines). The lower left histograms give the contribution of slingshots to the mass function in the two cases considered. Error bars are 1σ Poissonian noise. The nuclear SMBHs in these halos have masses $m_{\text{BH}} = (3.8 \pm 0.1) \times 10^6 M_{\odot}$ and $m_{\text{BH}} = (1.0 \pm 0.1) \times 10^8 M_{\odot}$, respectively.

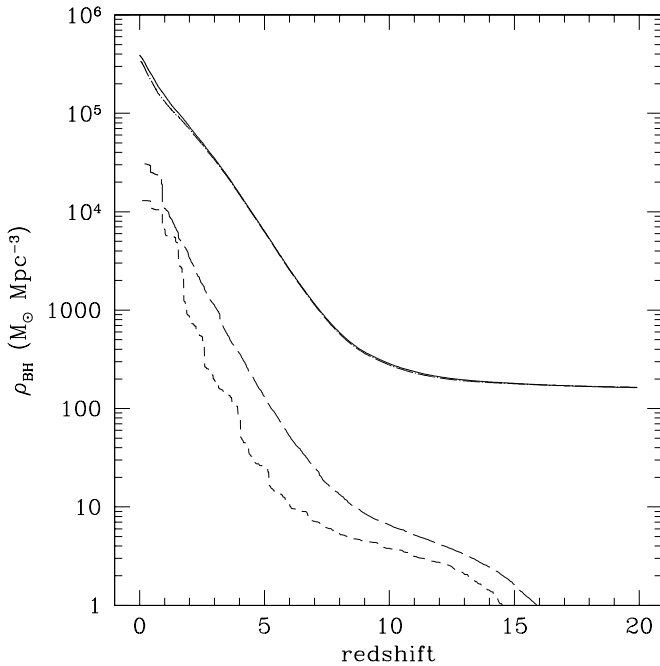


FIG. 14.—Contribution of nuclear, wandering, and intergalactic BHs to the mass density in BHs as a function of redshift. Solid line: Total mass density in all species. Dot-dashed line: Nuclear BHs. Long-dashed line: Wandering BHs retained in galaxy halos, most of them due to minor mergers. Short-dashed line: Single and binary BHs ejected in the IGM after a high-energy slingshot event.

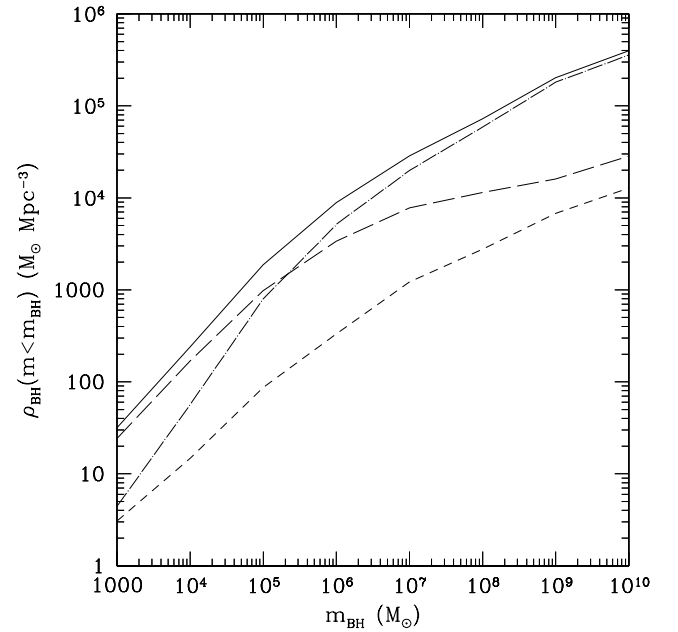


FIG. 15.—Cumulative mass density in BHs at redshift $z=0$. The total density is dominated by the nuclear BH contribution; however, the contribution of wandering BHs takes over for masses $\lesssim 10^5 M_{\odot}$. Solid line: Total mass density. Dot-dashed line: Nuclear BHs. Long-dashed line: Wandering BHs. Short-dashed line: Intergalactic BHs.

The cumulative local mass function of BHs is displayed in Figure 15. The heaviest BH hosted in a given DM halo has experienced several accretion episodes, lies in the nucleus, and has a well-defined mass according to the tight $m_{\text{BH}}-\sigma_c$ relation. Although the total mass in BHs is dominated, in every galaxy-sized halo, by the central hole, the same halo hosts a multiplicity of lighter wandering BHs, with masses ranging from $150 M_{\odot}$ to approximately one-tenth of the mass of the nuclear SMBH. Hence, the total BH mass density is dominated by wandering holes for masses $\lesssim 10^5 M_{\odot}$ and by nuclear ones above.

Note that on group and cluster scales our scheme would define “wandering” as all the nuclear BHs hosted in satellite galaxies, with only the BH of the central galaxy defined as “nuclear.” On the other hand, on galaxy scales, the cumulative mass contribution of wandering BHs is $\sim 10\%$ of the total (wandering+nuclear) mass in a given halo (Fig. 13). We extrapolate this fraction to larger scales, assuming that 10/11 of the wandering BH mass in groups and clusters is associated with nuclear BHs in satellite galaxies, and only 1/11 is due to true wandering holes. We have then re-adjusted the mass of wandering and nuclear BHs in groups and clusters accordingly.

We keep track of the positions of every single wandering hole within the host halos as it sinks to the center because of dynamical friction. The positions at the present epoch are typically spread between 0.1 and 0.6 of the virial radius. The large population of wandering BHs predicted by our model could be associated to the off-center ULXs observed in nearby galaxies (e.g., Colbert & Mushotzky 1999; Makishima et al. 2000; Kaaret et al. 2001).

4.4. Binary SMBHs and Quasars

The fraction of halos hosting nuclear BHs is shown in Figure 16. When computed over all branches of the merger

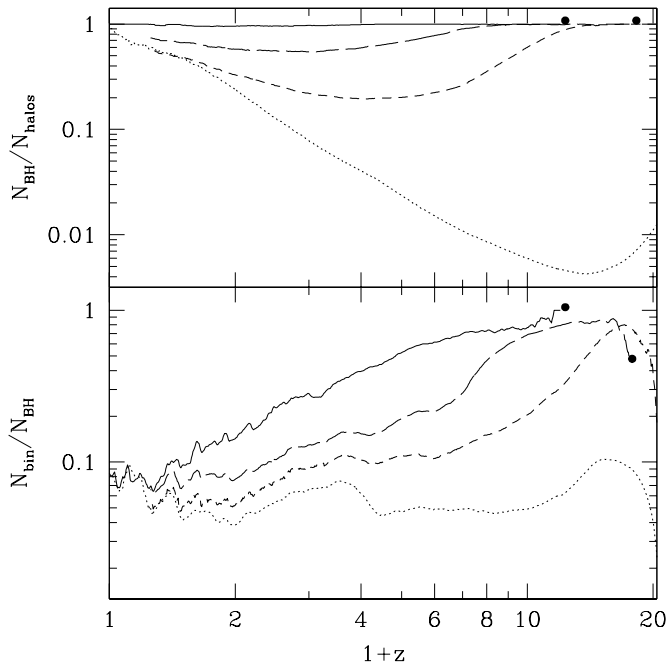


FIG. 16.—Fraction of halos hosting at least a nuclear SMBH vs. redshift (*upper panel*) computed weighting over all branches of the merger trees (*dotted curve*) and imposing different thresholds to the halo mass: $M > 10^{11} M_{\odot}$ (*solid curve*), $M > 10^{10} M_{\odot}$ (*long-dashed curve*), and $M > 10^9 M_{\odot}$ (*short-dashed curve*). The last two quantities are not plotted at $z < 0.25$, when the least massive halos in the merger trees are already above the adopted threshold. The mean SMBH occupation fraction is unity at the present epoch and, when weighted over all branches of the merger trees, drops below 10% at $z \geq 2$. Filled circles mark the epochs when sufficiently massive halos appear in the merger trees ($z \approx 11$ for $M > 10^{11} M_{\odot}$, $z \approx 16$ for $M > 10^{10} M_{\odot}$). Approximately 5%–10% of all nuclear BHs are in binaries (*lower panel*). This fraction increases with redshift in massive halos.

trees, i.e., considering at $z = 0$ only halos with $M > 10^{11} M_{\odot}$ with smaller and smaller halos appearing at higher redshifts, the occupation fraction depends on the assumed value of the resolution mass M_{res} . To avoid this problem, we compute the occupation fraction above a given minimum halo mass. As discussed by Menou et al. (2001), this fraction initially decreases with cosmic time as lower mass halos lacking nuclear BHs become more massive than the assumed threshold by successive mergers. Eventually, the occupation fraction starts to increase as the total number of individual halos drops. Note that our assumed “BH bias” (seed holes in 3.5σ peaks at $z = 20$) assures that all halos more massive than $10^{11} M_{\odot}$ actually host a BH at all epochs (triple interactions actually slightly reduce the occupation fraction somewhat below unity). In Figure 16 we also plot the fraction of all halos containing a nuclear BH that actually harbors a binary system. Summed all over the branches of the tree, this fraction is $\approx 5\%$ – 10% today. Almost all massive halos at early epochs host a binary, and eventually the fraction of binaries decreases with cosmic time because of coalescence.

A fraction $\approx 60\%$ of SMBH binaries at $z = 0$ have separation larger than 0.1 kpc and are still “soft,” while $\approx 10\%$ are in an advanced stage of hardening ($a < 10$ pc). The fraction of binaries strongly depends upon the total coalescence timescale, which, as discussed in § 3.4, is rather uncertain. We have then run a set of simulations with a stellar density

artificially decreased by a factor of 2, which implies a slower hardening rate by a factor of ~ 5 , on average. In this case triple interactions are more common because of the increased probability of having a binary still in the process of shrinking when a third intruder BH comes along. As a consequence, at low redshift ($z \lesssim 0.1$), the fraction of binaries becomes as large as 20%. The increased number of binaries is formed by close systems ($a < 10$ pc), hosted in galaxies that have not experienced any recent major merger.

Binary quasars are an intrinsically rare phenomenon, as both SMBHs must be active at the same time. Observationally, 16 pairs are known in a sample of $\sim 10^4$ QSOs, and among these 16 the confirmed physical associations are less than 10 (Kochanek, Falco, & Muñoz 1999; Mortlock, Webster, & Francis 1999; Junkkarinen et al. 2001). In our scheme, since only the SMBH hosted in the larger halo accretes and radiates during a major merger, at least two subsequent major mergers are required to give origin to a binary QSO system, the satellite BH being activated in the first merger event. Note that the mean timescale over which BHs accrete and radiate is $\sim 4 \times 10^7$ yr, much shorter than the typical time between two major mergers (Somerville et al. 2001). In our simulations we find a fraction of binary quasars with $L > 0.01 L_*$ that are $\approx (1-3) \times 10^{-3}$ at $z < 4$. A similar fraction is found taking a luminosity threshold of $0.1 L_*$ (L_* was calculated at every redshift from the polynomial evolution given by Boyle et al. 2000). If, instead, both BHs involved in a major merger were assumed to accrete, the fraction of binary quasars would be 2 orders of magnitude larger, in conflict with the existing data.

5. SUMMARY

Motivated by the recent discovery of luminous quasars around redshift $z \approx 6$ —suggesting a very early assembly epoch—and by numerical simulations of the fragmentation of primordial molecular clouds in cold dark matter cosmologies, we have assessed a model for the growth of SMBHs in the nuclei of luminous galaxies out of accreting Population III seed holes of intermediate masses, the end-product of the first generation of stars in (mini)halos collapsing at $z \sim 20$ from high- σ density fluctuations. As these pregalactic BHs become incorporated through a series of mergers into larger and larger halos, they sink to the center because of dynamical friction, accrete a fraction of the gas in the merger remnant to become supermassive, form a binary system, and eventually coalesce. We have followed the merger history of dark matter halos and associated BHs through cosmological Monte Carlo realizations of the merger hierarchy from early times until the present in a Λ CDM cosmology. In our scheme, the current mass of SMBHs lurking at the center of galaxy accumulates mainly via gas accretion, with BH-BH mergers playing only a secondary role.

The main results of our investigations can be summarized as follows:

1. A simple model where quasar activity is driven by major mergers and SMBHs accrete at the Eddington rate a mass that scales with the fifth power of the circular velocity of the host halo can reproduce the observed luminosity function of optically selected quasars in the redshift range $1 < z < 5$.
2. Hardening of BH binaries takes place efficiently both as a result of cuspy stellar density profiles that are replen-

ished after every major merger and, to some extent, due to triple BH interactions.

3. Although our seed BHs at $z = 20$ are very rare (one in every halo collapsing from 3.5σ density peaks), the nuclear SMBH occupation fraction is on the order of unity at the present epoch. It drops to less than 10% only at $z \geq 2$. Had we placed seed BHs in the 4σ density peaks instead, the occupation fraction of nuclear SMBH would be approximately 0.6 today.

4. The local fraction of binary SMBHs is on the order of 10%, with half of these systems having a separation larger than 100 pc. (Surviving binary SMBHs have mass ratios 0.2 ± 0.1 .) This fraction increases with redshift, so that almost all massive nuclear BHs at early epochs are in binary systems.

5. At $z < 4$, binary quasars represent a fraction $(1-3) \times 10^{-3}$ of all AGNs more luminous than $0.1 L_*$.

6. The long dynamical friction timescales and BH slingshots create a population of BHs wandering in galaxy halos and free-floating in the IGM, and contributing $\lesssim 10\%$ to the total BH mass density today. For a Milky Way-sized galaxy we estimate $\simeq 10$ wandering BHs with mass between 150 and 1000 M_\odot and ~ 1 wandering SMBH with $10^5 < m_{\text{BH}} < 10^6$

M_\odot (cf. MR01). For a halo with $\sigma_{\text{DM}} = 200 \text{ km s}^{-1}$ the number of wandering BHs is approximately 10 times larger.

Because of the sensitivity of our calculations on a number of uncertain parameters, these predictions should be regarded only as trends. Yet we believe our results shed new light on models for the assembly of SMBHs that trace their hierarchical buildup far up in the dark halo merger tree. In a subsequent paper we will explore in detail the possibility that the damage done to stellar cusps by binary BHs may be *cumulative*, together with the detectability of wandering BHs in galaxy halos, free-floating holes in the IGM, and coalescing SMBHs by a low-frequency gravitational wave experiment such as the planned *Laser Interferometer Space Antenna* (LISA).

We have benefitted from discussions with L. Ciotti, M. Colpi, D. Merritt, J. Ostriker, M. Rees, and G. Taffoni. Support for this work was provided by NASA through grants NAG5-4236 and NAG5-11513 (P. M.), by NSF grant AST-0205738 (P. M.), and by ASI (M. V.). M. V. thanks the Department of Astronomy and Astrophysics, University of California, Santa Cruz, for kind hospitality.

REFERENCES

- Abel, T., Bryan, G., & Norman, M. 2000, *ApJ*, 540, 39
 Adams, F. C., Graff, D. S., & Richstone, D. O. 2001, *ApJ*, 551, L31
 Bahcall, J. N., & Wolf, R. A. 1976, *ApJ*, 209, 214
 Bardeen, J. M., Bond, J. R., Kaiser, N., & Szalay, A. S. 1986, *ApJ*, 304, 15
 Barger, A. J., Cowie, L. L., Mushotzky, R. F., & Richards, E. A. 2001, *AJ*, 121, 662
 Barnes, J. E. 1988, *ApJ*, 331, 699
 Begelman, M. C., Blandford, R. D., & Rees, M. J. 1980, *Nature*, 287, 307
 Binney, J., & Tremaine, S. 1987, *Galactic Dynamics* (Princeton: Princeton Univ. Press)
 Bower, R. G. 1991, *MNRAS*, 248, 332
 Boyle, B. J., Shanks, T., Croom, S. M., Smith, R. J., Miller, L., Loaring, N., & Heymans, C. 2000, *MNRAS*, 317, 1014
 Bromm, V., Coppi, P. S., & Larson, R. B. 1999, *ApJ*, 527, L5
 ———. 2002, *ApJ*, 564, 23
 Bromm, V., Kudritzki, R. P., & Loeb, A. 2001, *ApJ*, 552, 464
 Burkert, A., & Silk, J. 2001, *ApJ*, 554, L151
 Carr, B. J., Bond, J. R., & Arnett, W. D. 1984, *ApJ*, 277, 445
 Carroll, S. M., Press, W. H., & Turner, E. L. 1992, *ARA&A*, 30, 499
 Cattaneo, A., Haehnelt, M. G., & Rees, M. J. 1999, *MNRAS*, 308, 77
 Cavaliere, A., & Vittorini, V. 2000, *ApJ*, 543, 599
 Ciotti, L., & van Albada, T. S. 2001, *ApJ*, 552, L13
 Colbert, E. J. M., & Mushotzky, R. F. 1999, *ApJ*, 519, 89
 Cole, S., Lacey, C. G., Baugh, C. M., & Frenk, C. S. 2000, *MNRAS*, 319, 168
 Colpi, M., Mayer, L., & Governato, F. 1999, *ApJ*, 525, 720
 Colpi, M., Possenti, A., & Gualandris, A. 2002, *ApJ*, 570, L85
 Eke, V. R., Cole, S., & Frenk, C. S. 1996, *MNRAS*, 282, 263
 Eke, V. R., Navarro, J. F., & Frenk, C. S. 1998, *ApJ*, 503, 569
 Faber, S. M., et al. 1997, *AJ*, 114, 1771
 Fan, X., et al. 2001a, *AJ*, 121, 54
 ———. 2001b, *AJ*, 122, 2833
 Ferrarese, L. 2002, *ApJ*, 578, 90
 Ferrarese, L., & Merritt, D. 2000, *ApJ*, 539, L9
 Fitchett, M. J. 1983, *MNRAS*, 203, 1049
 Fitchett, M. J., & Detweiler, S. L. 1984, *MNRAS*, 211, 933
 Fryer, C. L., Woosley, S. E., & Heger, A. 2001, *ApJ*, 550, 372
 Fuller, T. M., & Couchman, H. M. P. 2000, *ApJ*, 544, 6
 Gebhardt, K., et al. 2000, *ApJ*, 543, L5
 Ghigna, S., Moore, B., Governato, F., Lake, G., Quinn, T., & Stadel, J. 1998, *MNRAS*, 300, 146
 Gould, A., & Rix, H. 2000, *ApJ*, 532, L29
 Gross, M. A. K., Somerville, R. S., Primack, J. R., Holtzmann, J., & Klypin, A. 1998, *MNRAS*, 301, 81
 Haehnelt, M. G., & Kauffmann, G. 2000, *MNRAS*, 318, L35
 Haiman, Z., Abel, T., & Rees, M. J. 2000, *ApJ*, 534, 11
 Haiman, Z., & Loeb, A. 2001, *ApJ*, 552, 459
 Harms, R. J., et al. 1994, *ApJ*, 435, L35
 Hawking, S. W., & Ellis, G. F. R. 1973, *The Large-Scale Structure of Space-Time* (Cambridge: Cambridge Univ. Press)
 Hernquist, L. 1992, *ApJ*, 400, 460
 Hills, J. G., & Fullerton, L. W. 1980, *AJ*, 85, 1281
 Hut, P., & Rees, M. J. 1992, *MNRAS*, 259, P27
 Jang-Condell, H., & Hernquist, L. 2001, *ApJ*, 548, 68
 Junkkarinen, V., Shields, G. A., Beaver, E. A., Burbidge, E. M., Cohen, R. D., Hamann, F., & Lyons, R. W. 2001, *ApJ*, 549, L155
 Kaaret, P., et al. 2001, *MNRAS*, 321, L29
 Kauffmann, G., & Haehnelt, M. G. 2000, *MNRAS*, 311, 576
 Kochanek, C. S., Falco, E. E., & Muñoz, J. A. 1999, *ApJ*, 510, 590
 Koopmans, L. V. E., & Treu, T. 2003, *ApJ*, in press
 Lacey, C., & Cole, S. 1993, *MNRAS*, 262, 627
 Larson, R. B. 1998, *MNRAS*, 301, 569
 Madau, P., Ferrara, A., & Rees, M. J. 2001, *ApJ*, 555, 92
 Madau, P., & Rees, M. J. 2001, *ApJ*, 551, L27 (MR01)
 Magorrian, J., et al. 1998, *AJ*, 115, 2285
 Makishima, K., et al. 2000, *ApJ*, 535, 632
 Menou, K., Haiman, Z., & Narayanan, V. K. 2001, *ApJ*, 558, 535
 Merritt, D. 2000, in *ASP Conf. Ser. 197, Dynamics of Galaxies: From the Early Universe to the Present*, ed. F. Combes, G. A. Mamon, & V. Charmandaris (San Francisco: ASP), 221
 Merritt, D., & Ferrarese, L. 2001, *ApJ*, 547, 140
 Mihos, J. C., & Hernquist, L. 1994, *ApJ*, 425, L13
 ———. 1996, *ApJ*, 464, 641
 Milosavljevic, M., & Merritt, D. 2001, *ApJ*, 563, 34
 Mortlock, D. J., Webster, R. L., & Francis, P. J. 1999, *MNRAS*, 309, 836
 Nakamura, T. T., & Suto, Y. 1997, *Prog. Theor. Phys.*, 97, 49
 Peters, P. C. 1964, *Phys. Rev. B*, 136, 1224
 Omukai, K., & Nishi, R. 1998, *ApJ*, 508, 141
 Quinlan, G. D. 1996, *NewA*, 1, 35
 Quinlan, G. D., & Hernquist, L. 1997, *NewA*, 2, 533
 Richstone, D., et al. 1998, *Nature*, 395, 14
 Ripamonti, E., Haardt, F., Ferrara, A., & Colpi, M. 2002, *MNRAS*, 334, 401
 Rosati, P., et al. 2002, *ApJ*, 566, 667
 Salucci, P., Szuszkiewicz, E., Monaco, P., & Danese, L. 1999, *MNRAS*, 307, 637
 Schneider, R., Ferrara, A., Natarajan, P., & Omukai, K. 2002, *ApJ*, 571, 30
 Sheth, R. K., & Tormen, G. 1999, *MNRAS*, 308, 119
 Silk, J., & Rees, M. J. 1998, *A&A*, 331, L1
 Somerville, R. S., & Kolatt, T. S. 1999, *MNRAS*, 305, 1
 Somerville, R. S., Lemson, G., Kolatt, T. S., & Dekel, A. 2000, *MNRAS*, 316, 479
 Somerville, R. S., Primack, J. R., & Faber, S. M. 2001, *MNRAS*, 320, 504
 Sugiyama, N. 1995, *ApJS*, 100, 281
 Tormen, G. 1997, *MNRAS*, 290, 411
 Tremaine, S., et al. 2002, *ApJ*, 574, 740
 van den Bosch, F. C., Lewis, G. F., Lake, G., & Stadel, J. 1999, *ApJ*, 515, 50
 Wyithe, S., & Loeb, A. 2002, *ApJ*, 581, 886
 Xu, G., & Ostriker, J. P. 1994, *ApJ*, 437, 184
 Yu, Q. 2002, *MNRAS*, 331, 935
 Yu, Q., & Tremaine, S. 2002, *MNRAS*, 335, 965